

1 **Long-Term Follow-Up Defines the Population That Benefits from Early**
2 **Interception in a High-Risk Smoldering Multiple Myeloma Clinical Trial Using the**
3 **Combination of Ixazomib, Lenalidomide, and Dexamethasone.**

4
5 Running/Short title: Ixazomib, Lenalidomide, Dexamethasone in HR-SMM
6

7
8 Authors: Omar Nadeem^{1*}, Michelle P. Aranha^{1,4*}, Robert Redd², Michael Timonian^{1,4},
9 Sophie Magidson¹, Elizabeth D. Lightbody^{1,4}, Jean-Baptiste Alberge^{1,4}, Luca Bertamini¹,
10 Ankit K. Dutta¹, Habib El-Khoury¹, Mark Bustoros^{1,3}, Jacob P. Laubach¹, Giada Bianchi¹,
11 Elizabeth O'Donnell¹, Ting Wu⁴, Junko Tsuji⁴, Kenneth Anderson¹, Gad Getz⁴, Lorenzo
12 Trippa², Paul G. Richardson¹, Romanos Sklavenitis-Pistofidis^{1,4}, and Irene M. Ghobrial¹
13

14 ¹Center for Early Detection and Interception of Blood Cancers, Department of Medical
15 Oncology, Dana-Farber Cancer Institute, Boston, MA, USA

16 ²Department of Biostatistics and Computational Biology, Dana-Farber Cancer Institute,
17 Boston, MA, USA

18 ³Division of Hematology and Medical Oncology, Meyer Cancer Center, New York-
19 Presbyterian Hospital, New York, New York, USA

20 ⁴ Broad Institute, Boston, MA, USA
21

22 *Co-first author
23

24 Corresponding Authors:

25 Irene Ghobrial, MD
26 Dana-Farber Cancer Institute
27 450 Brookline Ave,
28 Boston, MA
29 irene_ghobrial@dfci.harvard.edu
30 Phone: 617-632-4198
31

Omar Nadeem, MD
Dana-Farber Cancer Institute
450 Brookline Ave,
Boston, MA
omar_nadeem@dfci.harvard.edu
Phone: 617-632-4952

32 Abstract

33 **Background:** Early therapeutic intervention in high-risk SMM (HR-SMM) has
34 demonstrated benefit in previous studies of lenalidomide with or without dexamethasone.
35 Triplets and quadruplet studies have been examined in this same population. However,
36 to date, none of these studies examined the impact of depth of response on long-term
37 outcomes of participants treated with lenalidomide-based therapy, and whether the use
38 of the 20/2/20 model or the addition of genomic alterations can further define the
39 population that would benefit the most from early therapeutic intervention. Here, we
40 present the results of the phase II study of the combination of ixazomib, lenalidomide,
41 and dexamethasone in patients with HR-SMM with long-term follow-up and baseline
42 single-cell tumor and immune sequencing that help refine the population to be treated for
43 early intervention studies.

44 **Methods:** This is a phase II trial of ixazomib, lenalidomide, and dexamethasone (IRD) in
45 HR-SMM. Patients received 9 cycles of induction therapy with ixazomib 4mg on days 1,
46 8, and 15; lenalidomide 25mg on days 1-21; and dexamethasone 40mg on days 1, 8, 15,
47 and 22. The induction phase was followed by maintenance with ixazomib 4mg on days 1,
48 8, and 15; and lenalidomide 15mg d1-21 for 15 cycles for 24 months of treatment. The
49 primary endpoint was progression-free survival after 2 years of therapy. Secondary
50 endpoints included depth of response, biochemical progression, and correlative studies
51 included single-cell RNA sequencing and/or whole-genome sequencing of the tumor and
52 single-cell sequencing of immune cells at baseline.

53 **Results:** Fifty-five patients, with a median age of 64, were enrolled in the study. The
54 overall response rate was 93%, with 31% of patients achieving a complete response and
55 45% achieving a very good partial response or better. The most common grade 3 or
56 greater treatment-related hematologic toxicities were neutropenia (16 patients; 29%),
57 leukopenia (10 patients; 18%), lymphocytopenia (8 patients; 15%), and thrombocytopenia
58 (4 patients; 7%). Non-hematologic grade 3 or greater toxicities included
59 hypophosphatemia (7 patients; 13%), rash (5 patients; 9%), and hypokalemia (4 patients;
60 7%). After a median follow-up of 50 months, the median progression-free survival (PFS)
61 was 48.6 months (95% CI: 39.9 – not reached; NR) and median overall survival has not
62 been reached. Patients achieving VGPR or better had a significantly better progression-
63 free survival ($p < 0.001$) compared to those who did not achieve VGPR (median PFS 58.2
64 months vs. 31.3 months). Biochemical progression preceded or was concurrent with the
65 development of SLiM-CRAB criteria in eight patients during follow-up, indicating that
66 biochemical progression is a meaningful endpoint that correlates with the development of
67 end-organ damage. High-risk 20/2/20 participants had the worst PFS compared to low-
68 and intermediate-risk participants. The use of whole genome or single-cell sequencing of
69 tumor cells identified high-risk aberrations that were not identified by FISH alone and
70 aided in the identification of participants at risk of progression. scRNA-seq analysis
71 revealed a positive correlation between MHC class I expression and response to
72 proteasome inhibition and at the same time a decreased proportion of GZMB+ T cells
73 within the clonally expanded CD8+ T cell population correlated with suboptimal response.

74 **Conclusions:** Ixazomib, lenalidomide and dexamethasone in HR-SMM demonstrates
75 significant clinical activity with an overall favorable safety profile. Achievement of VGPR
76 or greater led to significant improvement in time to progression, suggesting that achieving
77 deep response is beneficial in HR-SMM. Biochemical progression correlates with end-
78 organ damage. Patients with high-risk FISH and lack of deep response had poor
79 outcomes. ClinicalTrials.gov identifier: (NCT02916771)

80

81 Funding: Takeda and Celgene (Bristol Myers Squibb) provided support for the clinical
82 trial. These funders reviewed the final manuscript and approved its publication; they were
83 not involved in the conceptualization, design, data collection, analysis, or preparation of
84 the manuscript. Funding was also provided by the Dr. Miriam and Sheldon G. Adelson
85 Medical Research Foundation and the NIH (R35CA263817 awarded to I.M.G.).

86

87 Introduction

88
89 Smoldering multiple myeloma (SMM), defined by the presence of $\geq 10\%$ clonal plasma
90 cells in the bone marrow and/or $\geq 3\text{g/dl}$ monoclonal (M) protein in the serum without the
91 presence of any myeloma-defining events (MDE), carries a heterogeneous risk of
92 progression to overt multiple myeloma (MM), with an average risk of 10% per year for the
93 first 5 years after diagnosis and then approximately 1-2% per year thereafter¹. There is a
94 subset of patients that are considered high-risk SMM (HR-SMM) and multiple efforts have
95 been undertaken to further define this high-risk group, which carries an approximately
96 50% risk of progression to overt MM at 2 years. The Mayo 2008 criteria defined HR-SMM
97 as having $\geq 10\%$ plasmacytosis, M protein $\geq 3\text{ g/dl}$, and an SFLC ratio ≥ 8 or ≤ 0.125 ².
98 Many additional risk models have been studied including the PETHEMA criteria, evolving
99 criteria, and IgA subtype, all of which were also shown to have prognostic relevance³. A
100 study by Rajkumar et al. compiled all the high-risk features of SMM to help define this
101 population⁴. Later, the IMWG/Mayo 2018 criteria were revised and defined high risk as
102 having the presence of at least 2 of the following 3 criteria: bone marrow plasmacytosis
103 $>20\%$, M protein $>2\text{ g/dl}$, and an SFLC ratio >20 ^{5,6}. While these models help identify
104 patients at high risk of progression, they mostly leverage clinical variables and can give
105 discordant results for an individual⁷. Prediction models that take into account disease
106 biology may be able to overcome some of these challenges. In recent years for example,
107 *MYC* translocations and copy number abnormalities, *KRAS* mutations, Del17p and *TP53*
108 mutations, as well as APOBEC activity and chromothripsis have been shown to portend
109 a higher risk of progression⁸⁻¹².

110
111 Management of SMM has historically consisted of observation. However, with advances
112 in risk stratification methods and MM therapy, early therapeutic intervention may offer an
113 improved prognosis without morbidity from MM for high-risk patients. There have been 2
114 phase III trials utilizing lenalidomide or lenalidomide and dexamethasone in patients with
115 HR-SMM. Both studies demonstrated improvement in progression-free survival (PFS),
116 and one also demonstrated improvement in overall survival, further arguing for early
117 intervention^{13,14}. While the prolongation of overall survival with early intervention is a
118 subject of debate, prolonging progression-free survival may delay end-organ damage
119 which can be irreversible and can severely impact a patient's quality of life¹⁵⁻¹⁷.

120
121 Following these two randomized studies, multiple phase II studies using triplet or more
122 recently quadruplet therapy have been initiated in high-risk SMM¹⁸⁻²¹. However, there are
123 many unresolved questions about the optimal management of patients with HR-SMM,
124 particularly regarding the use of response assessment metrics that were originally
125 developed in patients with overt MM, such as depth of response and biochemical
126 progression, as well as determining the group of patients who may benefit the most from
127 early intervention. The studies using lenalidomide with or without dexamethasone had
128 low rates of complete response and therefore could not assess the role of depth of
129 response in long-term follow-up. Additionally, more recent studies using quadruplet
130 therapy do not have enough long-term follow-up to assess this question yet. Here, we
131 used the combination of ixazomib, lenalidomide, and dexamethasone in high-risk SMM.
132 We aimed to help address several critical questions for therapeutic intervention in HR-

133 SMM: 1) whether depth of response (VGPR or CR) matters in the long-term outcome of
134 patients treated with a lenalidomide-based therapy, 2) whether biochemical progression
135 correlates with end-organ damage, 3) whether 20/2/20 defines participants who would
136 benefit the most from early intervention with lenalidomide-based therapy, and 4) whether
137 the addition of genomic biomarkers can improve the risk stratification of these participants
138 enrolled on these studies.

139

140

141 Results

142

143 Baseline characteristics.

144

145 Between March 2017 and February 2020, 55 patients were enrolled on this study (**Figure**
146 **1A**). Patient baseline characteristics, definition of high-risk SMM, and high-risk
147 cytogenetics are summarized in **Table 1A**. The median age was 64 (range 40-84) with
148 30 (55%) males and 25 (45%) females. All patients had an Eastern Cooperative Oncology
149 Group (ECOG) performance status of ≤ 1 . Patients were enrolled using the list of high-risk
150 criteria compiled by Rajkumar et al⁴. For cross-study comparisons, we defined patients
151 with high-risk disease based on several validated models in **Table 1B**, including the Mayo
152 2008, Mayo 2018, IMWG risk score tool, and high-risk cytogenetics. High risk FISH was
153 defined as follows: gain1q, del13q, del17p, del1p, t(4;14), t(14;16).

154

155 While FISH testing is a standard method to define risk in MM, the failure rate of FISH in
156 this study was 36% (FISH at screening was successful in 35/55) (**Figure 1B**). Therefore,
157 we employed whole genome sequencing (WGS) and single-cell RNA (scRNA)
158 sequencing to identify high-risk translocations and copy number alterations (CNA). The
159 translocations and copy number alterations identified by FISH, WGS, and scRNA-seq are
160 displayed in **Figure 1B**. From scRNA-seq, we leveraged the expression level of primary
161 IgH translocation marker genes to infer the presence of translocations and observed high
162 concordance between the expression of said marker genes and FISH results, but
163 additionally detected translocations in three patients in whom FISH had failed due to low
164 cell numbers. Furthermore, using Numbat²² to infer CNAs from scRNA-seq data, we
165 detected hyperdiploidy (homologous recombination deficiency: HRD) in another four
166 patients in whom FISH had failed due to low cell numbers, as well as additional high-risk
167 secondary CNVs such as Amp1q, Del13q, and Del1p in four patients. Whole-genome
168 sequencing confirmed the IgH translocations, hyperdiploidy, and secondary CNVs in 10
169 patients with both WGS and scRNA-seq of tumor cells. No discrepancies were observed
170 between scRNA-seq and WGS. Overall, for ten patients where FISH failed due to a low
171 number of cells, scRNA-seq and WGS data existed and we were able to resolve the
172 cytogenetic abnormalities for these cases. Notably, the first aspirate pull was used for
173 clinical-grade FISH testing, while later pulls were used for research-level WGS and
174 scRNA-seq; given the frequent hemodilution observed in later aspirate pulls which further
175 decreases the number of tumor cells in the specimen, these results showcase the
176 superior sensitivity in tumor cell detection and characterization of these methods
177 compared to FISH. Further, by reviewing pre-screening FISH reports and incorporating
178 primary translocation data from treatment records for remaining failures, we obtained

179 cytogenetic data for 49 out of 55 individuals. Since we did not have whole-exome
180 sequencing or WGS data on all patients, we refrained from assessing the impact on
181 outcomes of certain high-risk mutations, including MAPK mutations, DNA repair
182 mutations, or MYC alterations, which have been previously identified as high risk^{8,10,12}.

183 Safety

184 Toxicity results are summarized in **Table 2**. Thirty-six percent of patients experienced a
185 grade 2 toxicity, 62% experienced a grade 3 toxicity and 9% experienced a grade 4
186 toxicity. The most common treatment-related toxicities of any grade included leukopenia
187 in 44 patients (80%), neutropenia in 43 patients (78%), fatigue in 42 patients (76%), rash
188 in 38 patients (69%), and diarrhea in 37 patients (67%). The most common grade 3
189 treatment-related hematologic toxicities were neutropenia in 14 patients (25%),
190 leukopenia in 10 patients (18%), lymphopenia in 6 patients (11%), and thrombocytopenia
191 in 4 patients (7%). Non-hematologic grade 3 toxicities included hypophosphatemia in 7
192 patients (13%) and rash in 5 patients (9%). Grade 4 toxicities related to study treatment
193 included hyperglycemia (n = 1/55; 2%), hypokalemia (n = 1/55; 2%), lymphopenia (n =
194 2/55; 4%), neutropenia (n = 2/55; 4%), and thrombocytopenia (n = 1/55; 2%). One patient
195 developed a grade 5 intracranial hemorrhage 3 weeks after completion of therapy that
196 was not related to the study intervention; the patient was on therapeutic anticoagulation
197 with a history of atrial fibrillation and the event was considered unrelated by the patient's
198 treating physicians.

199 Five patients developed secondary malignancies (one instance each of prostate,
200 head/neck, ovarian, uterine and melanoma). Three of five patients were diagnosed
201 following the completion of treatment on protocol and remained on follow-up while
202 receiving active treatment for secondary malignancy. The remaining two patients were
203 diagnosed during active treatment; one participant delayed treatment for secondary
204 malignancy (prostate) to finish protocol therapy and remained on study through the end
205 of protocol-based follow-up. The other patient diagnosed during active treatment
206 discontinued therapy to receive treatment for their secondary malignancy (melanoma)
207 and remained on follow-up. No patients were diagnosed with myelodysplastic syndrome
208 or other myeloid malignancies.

209 Dose modifications occurred in 34 patients (62%) during the study therapy. The median
210 number of modifications was 1 (range 1-4) and dose delays due to toxicity occurred in 19
211 patients (35%). The most common reason for dose modification of ixazomib was
212 peripheral neuropathy (10 patients, 18%). Stem cells were collected from all eligible
213 patients by the end of the induction phase and there was one patient who failed to
214 mobilize stem cells.

215 The median number of cycles completed was 24 (range: 2-24). Five patients discontinued
216 therapy prior to the planned 24 cycles. Reasons for discontinuation included worsening
217 unrelated co-morbid conditions (n=3), treatment for a different malignancy (n=1), and
218 withdrawal of consent (n=1). No patients discontinued treatment due to toxicity.

219 Efficacy

220 The overall response rate (partial response or better) based on International Myeloma
221 Working Group (IMWG) criteria²³ was 93% (n=51), with complete response (CR)
222 observed in 17 patients (31%), VGPR in 8 patients (15%), and partial response in 26
223 patients (47%) (**Table 3**). All patients who achieved CR also achieved a stringent and
224 sustained CR for at least 6 months with responses deepening over time (**Figure 2**).
225 Twenty-five patients (45%) achieved a VGPR or better response and minimal response
226 or better was observed in 98% of patients (n=54). The overall response rate was similar
227 for patients in different 20/20 risk groups: low (100%), intermediate (90%), and high
228 (92%) (Cochran-Armitage test, p=0.55).

229 Eight participants progressed to overt MM defined by the SLiM-CRAB myeloma-defining
230 events (MDEs)²⁴ (**Figure 2**). All eight patients experienced biochemical progression
231 concurrent with or prior to developing SLiM-CRAB progression (**Figure 2**). One patient
232 discontinued protocol therapy after one cycle due to unrelated comorbid conditions
233 including colitis and atrial fibrillation and remained on follow-up for ten months prior to
234 SLiM-CRAB progression. The remaining seven progressors completed all twenty-four
235 cycles of protocol therapy and continued on follow-up prior to progression. Four of eight
236 progressors had an MDE within one year of their final treatment, and the median time to
237 progression for the remaining four progressors was 21 months (range: 13.2-32.7 months).
238 Four patients developed lytic bone disease noted on PET and MRI during follow-up, one
239 patient developed renal failure and hypercalcemia 9 months after completion of therapy
240 (after showing biochemical progression at 6 months post-therapy), one patient developed
241 anemia 17 months post-therapy after showing biochemical progression at 6 months post-
242 therapy, one patient met SLiM-CRAB criteria at 13 months post-therapy with FLC ratio >
243 100 and BMPCs of 60% prompting initiation of therapy and one patient met SLiM-CRAB
244 criteria at 13 months post-therapy with FLC ratio >100. Seven of the eight had at least
245 one high-risk genetic event at baseline [1q gain (n=4), Del13q (n=5), Del17p (n=2, one
246 confirmed from FISH tests and one identified in a pre-screening FISH report from patient
247 records), Del1p (n=3), t(14;16) (n=1), KRAS (n=2), TP53 (n=1)] (**Figure 1B**). Among all
248 progressors, the best response achieved was PR with none achieving VGPR or better.

249

250 Time-to-event analyses

251 The median follow-up for all 55 patients was 50 months (range: 8-61 months). Thirty
252 patients had biochemical progression events (**Figure 2**). Biochemical progression was
253 defined as a 25% increase in serum or urine M protein or a difference between involved
254 and uninvolved FLC levels based on the IMWG criteria²⁵.

255 The total number of patients who were followed for at least two years and remained
256 biochemical progression-free (including the censored patients who came off therapy
257 with or without progression) was 50 of 55 patients (91%; 90% CI: 82 - 96%, p < 0.001,
258 one-sided exact binomial test) (**Figure 3A**).

259

260 Progression-free survival for the primary endpoint was defined as the development of
261 end-organ damage per the SLiM-CRAB criteria or death. Participants who were not
262 followed for at least two years, yet remained alive and progression-free while on trial,
263 were censored at the last date known progression-free. The total number of patients who
264 remained progression-free without SLiM-CRAB criteria or death within two years of
265 enrollment was 52 of 53 patients (98%) (**Figure 3B**). One patient developed SLiM-CRAB
266 progression within 2 years of enrollment after discontinuing therapy (described above).
267 No patients developed SLiM-CRAB progression while on active therapy (**Figure 3B**).

268 Median biochemical PFS was 48.6 months (95% CI: 39.9 – not reached; NR) and median
269 overall survival has not been reached (**Figure 3 A, C**). The median duration of response
270 was 47.4 months (95% CI: 37 – NR) and the median time to progression was 49.9 months
271 (95% CI: 39.9 – NR).

272 Subsequent treatments for those with biochemical progression but not SLiM-CRAB

273 Eleven patients started new treatments on SMM-directed clinical trials following the
274 completion of protocol therapy prior to the development of SLiM-CRAB progression. Of
275 these, ten experienced biochemical progression while on follow-up (**Figure 2**) and had
276 an evolving pattern leading to enrollment in a subsequent clinical trial. Evolving pattern
277 was defined as an increase of 10% in the M-spike concentration or the involved free light
278 chain concentration during the 6 months prior to screening for the clinical trial. Four
279 patients met high-risk criteria per the 20/2/20 model on follow-up. These patients elected
280 not to wait for end-organ damage on follow-up and proceeded with therapy on another
281 trial of HR-SMM.

282 Factors that impact progression-free survival

283 We next assessed several baseline characteristics to determine factors that define the
284 population that benefits the most from a lenalidomide-based regimen and further
285 identified endpoints that can be early biomarkers for end-organ damage in this population.
286 We examined baseline characteristics including the 20/2/20 model, evolving subtype,
287 high-risk cytogenetics, the best response to therapy, as well as the combination of
288 response, high-risk cytogenetics, and minimal residual disease (MRD). These criteria
289 were used based on their association with prognosis in prior studies of overt MM in a prior
290 post hoc assessment in lenalidomide studies of SMM^{26,27}.

291 We first determined whether the baseline 20/2/20 criteria helped identify patients who
292 would have a prolonged PFS in response to therapy. We combined low- and intermediate-
293 -risk patients and compared them to high-risk patients. Here, we showed that the median
294 PFS was longer but not statistically significant at 57.8 months for the low-/intermediate-
295 risk group compared to 37.2 months for high-risk patients (log-rank, $p = 0.08$) (**Figure**
296 **3D**). The median duration of response was significantly shorter at 31.6 months in high-
297 risk patients compared to 56.9 in the low/int group (log-rank, $p = 0.046$) (**Figure 3E**).

298 Evolving disease was assessed in all participants as part of the eligibility criteria and as
299 described above this was defined as a 10% or greater increase in either the M-spike
300 concentration or the involved free light chain concentration within the 6 months preceding
301 clinical trial screening. Of all patients that enrolled in the clinical trial (N=55), an evolving
302 pattern was found in 29 out of 55 patients (53%) while 26 out of the 55 patients (47%) did
303 not have an evolving pattern (**Table 1**). The median time of the lab result was 107 days
304 prior to the screening date with an interquartile range of 120 days. The presence of
305 evolving disease at baseline was similar across baseline IMWG 20/2/20 risk groups: low
306 (56%), intermediate (48%), and high (56%) (Cochran-Armitage, $p=0.83$). Of the patients
307 that demonstrated an evolving pattern, only 31% ($n=9/29$) achieved a VGPR or better,
308 and of those that did not demonstrate an evolving pattern, 62% ($n=16/26$) achieved a
309 VGPR or better (Fisher's exact, $p=0.032$).

310 In patients who did not demonstrate an evolving pattern, the PFS was significantly longer
311 at 53.4 months compared to 40.1 months in those who had evolving disease prior to
312 registration (log-rank, $p=0.025$). Additionally, in patients who did not demonstrate an
313 evolving pattern, the median duration of response was not reached and was significantly
314 longer compared to that in patients who had an evolving subtype (37.9 months; log-rank,
315 $p=0.034$) (**Figure 4A-D**).

316 We next examined whether patients with VGPR or CR had an improved progression-free
317 survival. Response has been associated with PFS in studies of overt MM²⁸. However, this
318 has not been previously shown in studies of smoldering myeloma partially because the
319 previous studies using lenalidomide and dexamethasone had few cases of CR and
320 partially for the short follow-up period of the quadruplet regimens being currently
321 assessed in SMM. We, therefore, aimed to determine whether depth of response is
322 associated with progression in the SMM setting. Indeed, we demonstrated that patients
323 who showed VGPR or better had a median time to progression (TTP) of 58.2 months
324 compared to 31.3 months in patients who showed inferior responses (log rank, $p < 0.001$;
325 **Figure 5 A**). Interestingly, this was still true in patients with high-risk cytogenetics as
326 determined by FISH only (median PFS 31.3 months vs 53.4 months, log-rank, $p = 0.002$)
327 or by FISH and whole genome sequencing(WGS) (median PFS of 30.8 months vs 53.4
328 months, $p < 0.001$), demonstrating that depth of response is relevant for prognostication
329 independent of cytogenetics (**Figure 5 B,C**).

330 All patients who achieved a complete response (CR) maintained it for at least 6 months.
331 The median duration of response in the sustained CR group was not reached at the time
332 of analysis, while the median duration of response in the non-CR group was 35.5 months
333 (log-rank, $p = 0.0016$) (**Figure 5D**). Similarly, the median progression-free survival in the
334 sustained CR group was not reached, compared to 38 months in the non-CR group (log-
335 rank, $p = 0.0018$) (**Figure 5E**).

336

337 Minimal Residual Disease

338 Twenty-five patients were evaluable for MRD (achieved VGPR or better) by next-
339 generation sequencing (NGS), 11 out of 25 had no samples available for MRD testing or
340 had a quality control (QC) failure. Twenty-three samples at C9 or EOT from 14 out of 25
341 patients passed the QC analysis and were available for MRD testing. A sensitivity of 10^{-5}
342 was reached in 22/23 (96%) samples and a sensitivity of 10^{-6} in 17/23 samples (74%)
343 (**Suppl Figure S1**). Out of patients who showed a VGPR or better response and had
344 MRD testing (n=14), 29% (4/14) were MRD negative at 10^{-5} at EOT and none developed
345 biochemical or clinical progression over the follow-up period. Of those who were MRD
346 positive at 10^{-5} (n=10/14), 6 patients developed biochemical progression during the follow-
347 up period. Two MRD time points (C9 and EOT) were available in a subgroup of 8
348 individuals. Of those, 50% (4/8) were MRD positive at 10^{-5} at C9 and remained so at EOT,
349 while 50% (4/8) were MRD negative at 10^{-5} at C9 but only 1 patient remained MRD
350 negative at EOT, and 3 converted to MRD positive. The 3 patients that converted from a
351 C9 MRD negative at a sensitivity of 10^{-5} to positive at EOT developed biochemical
352 progression during the follow-up period. The 5-year progression-free survival rate of
353 patients who achieved MRD negativity at 10^{-5} was 100%, compared to 40% of MRD-
354 positive patients (log-rank, $p = 0.051$) (**Figure 6**).

355 Mass Spectrometry MRD assessment

356 MALDI-TOF mass spectrometry was available at baseline and C9 in 43 patients. The M-
357 protein was undetectable in 4 patients at C9 (10%). Since clearance of M-protein could
358 take more time than tumor cell clearance in the BM, we tested the serum of patients by
359 MALDI-TOF in available serum samples during maintenance at 2-6 months after C9 (at
360 C11 to 16). 37 were retested during maintenance: six were negative (including the 4 that
361 were negative at C9) and 31 remained positive. At EOT, MALDI-TOF was performed for
362 41 patients. Eight (20%) were negative: 6 out of 8 confirmed a previous negative result,
363 one case turned negative from a previous positive result, and one had a negative result
364 from baseline with no testing during treatment. The concentration calculated using the
365 EXENTi software positively correlated with that calculated via SPEP at diagnosis, C9 and
366 EOT ($p < 0.0001$) (**Suppl Figure S3**). Of the patients with negative MALDI-TOF at EOT
367 (n=8), 4 developed biochemical progression, and none developed SLiM-CRAB
368 progression. In patients who achieved a negative MALDI-TOF result at EOT, the median
369 progression-free survival was 53.46 months compared to 38.01 months in patients who
370 had a positive MALDI-TOF result at EOT (log-rank, $p=0.08$) (**Suppl Figure S4**).

371
372 We compared residual disease detection using serum immunofixation (IFX) with MALDI-
373 TOF in 86 measurements. While both tests are significantly concordant (Table S1,
374 Cohen's $\kappa=0.64$, $p < 0.001$, 95% CI [0.44, 0.84]) and no patients had a positive IFX test
375 and a negative MALDI-TOF test, MALDI-TOF identified some cases missed by IFX (10
376 IFX-negative MALDI-TOF-positive cases). Therefore, MALDI-TOF might be more
377 sensitive than IFX for detecting residual disease.

378

379 **Single-cell RNA sequencing reveals tumor-intrinsic and extrinsic factors**
380 **associated with disease progression**

381
382 To identify biological predictors of response and resistance to IxaRD in baseline samples
383 from patients with HR-SMM, we performed single-cell RNA sequencing on CD138+ and
384 CD138- cells as well as WGS on 22 patients enrolled on the study (14 biochemical
385 progressors, 8 non-progressors) and 11 Healthy donors (**Figure 7A**). Among the
386 progressors in this subcohort, 5 patients met SLiM CRAB criteria (**Figure 7A**).

387
388 Overall, we identified 125,572 plasma cells (Patients: malignant, n=50,591; normal,
389 n=1876; HD: n=73,105) (**Figure 7B-D**). To identify tumor-intrinsic transcriptomic
390 alterations associated with biochemical progression post-IxaRD in patients with HRSMM,
391 we performed differential expression analysis comparing tumor cells from patients who
392 progressed (n=10) to those who did not (n=3). To restrict the influence of individual tumors
393 on the analysis, as well as to control for the lower number of non-progressors in this sub-
394 cohort, we randomly sampled the same number of tumor cells from progressors and non-
395 progressors (~2100 per group) and balanced the contribution of each individual towards
396 the group (progressors: ~210 cells per patient; non-progressors: 700 cells per patient;
397 **Figure 7E**). Additionally, to control for differences in sequencing depth, we downsampled
398 20K reads per cell across all cells used in this analysis. We observed consistently higher
399 expression levels of MHC class I genes (*HLA-A*, *HLA-B*, *HLA-F*, *HLA-E*, *B2M*) in tumor
400 cells from non-progressors to progressors (**Figure 7E**). To validate this observation, we
401 analyzed bulk RNA-sequencing data from an external cohort of MM patients treated with
402 a Bortezomib-based regimen, a different proteasome inhibitor (PADIMAC, GSE116234).
403 This analysis confirmed that tumor cells from patients who respond well to proteasome
404 inhibition show higher levels of MHC-I genes (**Figure 7F**). Notably, the PADIMAC study
405 did not use Lenalidomide in combination with proteasome inhibition, which was the case
406 in our study. This supports the notion that the observed association with MHC-I levels is
407 related to proteasome inhibition specifically rather than a particular combination.

408 These results suggest that antigen presentation via MHC-I by tumor cells may be
409 important for response to proteasome inhibition and implicate the immune system in
410 mediating response. While the immune system has been thought to potentiate the effects
411 of proteasome inhibition through increased neoantigen presentation by immune cells
412 following tumor cell killing, it has not been previously linked to tumor-intrinsic
413 transcriptomic alterations²⁹. To pursue this hypothesis further, we turned our attention to
414 the cytotoxic CD8+ T cell compartment, which is tasked with responding to MHC-I-bound
415 tumor-derived antigens. Overall, we sequenced 51,326 T-cells, including 5,045 granzyme
416 K (GZMK)-expressing and 9,026 granzyme B (GZMB)-expressing cytotoxic T cells
417 (**Figure 7G**). First, we systematically compared the frequency of clonal expansion within
418 the GZMK+ and the GZMB+ compartment between progressors and non-progressors.
419 We observed that the GZMK+ compartment was significantly more clonally expanded in
420 progressors compared to non-progressors (bootstrapping, two-sided p<0.001) (**Figure**
421 **7H**), but this was not seen in the GZMB+ compartment. By comparing the frequency of
422 the GZMB+ phenotype within clonally expanded T cells from progressors and non-
423 progressors, we observed a significant decrease in differentiation towards the GZMB+
424 phenotype in progressors (Wilcoxon, two-sided p=0.048) (**Figure 7 I, J**). This suggests

425 that clonally expanded effector cytotoxic T cells from progressors may be less mature
426 compared to non-progressors. To gain more insight into the functionality of clonally
427 expanded GZMB+ cytotoxic T cells, we performed differential expression analysis
428 between progressors and non-progressors. We observed that clonally expanded GZMB+
429 cytotoxic T cells from non-progressors showed higher expression levels of genes related
430 to cytotoxicity and activation, such as *TYROBP*, *CXCR4*, and members of the AP-1
431 pathway, compared to progressors (**Figure 7K**). Clonally expanded GZMB+ cytotoxic T
432 cells from progressors showed higher levels of GIMAP genes, which may be associated
433 with increased apoptosis³⁰, and *THEMIS*, which can suppress cytotoxic responses³¹,
434 however higher levels of maturation markers *ITGB1* and *CX3CR1* were also observed,
435 suggesting that the functionality of clonally expanded GZMB+ cytotoxic T cells may be
436 more nuanced.
437 Overall, this suggests that clonally expanded cytotoxic T cells from progressors are
438 phenotypically less mature, and potentially less functional, compared to those from non-
439 progressors, which could be related to the observed differences in MHC-I expression in
440 tumor cells. This data implicates immune dysfunction as a potential correlate of
441 suboptimal response to proteasome inhibition.

442 443 **Discussion**

444
445 Optimal management of HR-SMM continues to evolve with many novel approaches
446 currently under investigation to deliver highly effective therapy to prevent end-organ
447 damage while limiting toxicity. There have been phase III studies of lenalidomide and
448 dexamethasone demonstrating improvement in progression-free and overall survival and
449 there are ongoing studies utilizing triplets or quadruplets that include monoclonal
450 antibodies with proteasome inhibitors, lenalidomide, and dexamethasone. The ixazomib,
451 lenalidomide, and dexamethasone combination in this study demonstrated high response
452 rates with many patients experiencing deep responses, with VGPR or better in nearly half
453 of the patients treated as well as the benefit of an all-oral approach. No patients
454 progressed to overt MM during study therapy and the regimen was overall well-tolerated.
455 The response rates and safety were comparable to results seen in clinical trials of
456 ixazomib, lenalidomide, and dexamethasone of newly diagnosed and relapsed MM^{32,33}.
457 The median PFS of 48.9 months also compares favorably to previously reported clinical
458 trials of triplet combination regimens in SMM^{19,20}.

459
460 Because of the long follow-up of a median of 50 months and the depth of response
461 achieved in half of the patients, we have an opportunity to answer critical questions about
462 the management of early intervention in HR-SMM.

463
464 A controversial question in SMM trials is whether depth of response matters in trials of
465 HR-SMM. Previous studies using lenalidomide alone or lenalidomide and
466 dexamethasone demonstrated a long-term benefit and delay of end organ damage even
467 if the best response was only PR. The argument was that immune equilibrium may be re-
468 instated in those patients and deep remission is not required. However, other studies
469 using “curative intent” argued that achieving a depth of response similar to overt MM is
470 the most optimal way to achieve long-term remission. Here, we show for the first time that

471 a depth of response of VGPR or greater correlated with time to progression, suggesting
472 that deep response is impactful in SMM similar to overt MM. This was particularly
473 highlighted in patients with cytogenetically high-risk disease, where PFS was only 30.8
474 months in patients with less than VGPR.

475
476 The next question was whether MRD is associated with improved PFS. Although the
477 numbers were small, we were still able to see near-significant differences in the PFS of
478 MRD negative cases compared to those who did not achieve or sustain MRD negativity.
479 Ongoing studies with deeper remissions with quadruplet therapy or immunotherapy will
480 help further address this question more definitively.

481
482 We then examined the correlation of biochemical progression with the development of
483 SLiM-CRAB criteria. Thirty patients developed biochemical progression in all (27 after
484 completion of therapy), of which 8 patients also developed SLiM-CRAB with overt MM.
485 Eleven patients started new treatments on SMM-directed trials following the completion
486 of protocol therapy prior to developing SLiM-CRAB progression. Of these, ten
487 experienced biochemical progression while on follow-up and had an evolving pattern
488 leading to enrollment in a subsequent clinical trial. Four of these patients met high-risk
489 criteria per the 20/2/20 model. This is consistent with our clinical observation that patients
490 who opt to be treated initially for HR-SMM do not want to wait for the development of end-
491 organ damage prior to re-initiating therapy, consistent with recent discussions to consider
492 biochemical progression as an end-point of therapy rather than SLiM-CRAB³⁴. In addition,
493 it brings up a critical question of whether re-treatment on a trial of SMM should be in the
494 same cohort with other participants who were never exposed to therapy or in a separate
495 cohort. Additional guidance is necessary to determine which patients would be suitable
496 for further SMM-directed therapy vs MM induction therapy.

497
498 The strong correlation between biochemical progression and MDE also points out that
499 biochemical progression can be used as a surrogate for MDE in high-risk SMM. However,
500 the number of patients is small, and other studies need to further confirm this observation.

501
502 Interestingly, the use of 20/2/20 criteria in our study demonstrated that responses were
503 similar across all risk criteria, but the progression-free survival was shortest for those who
504 were high-risk per 20/2/20. This indicates that high-risk 20/2/20 patients may resemble
505 MM and may require more aggressive therapy or maintenance therapy. We did not have
506 an observation control arm in this study, so we cannot assess whether achieving
507 response in these patients truly alters their long-term risk of progression to MM.

508
509 Moreover, the use of evolving subtype helped capture those with increasing biomarkers
510 regardless of their disease burden. The best response to treatment was not similar in
511 those who showed increasing biomarkers prior to receiving therapy compared to those
512 who had fairly stable biomarkers. In patients who did not show an evolving disease pattern
513 as defined in our eligibility criteria, the best response to therapy achieved was better,
514 duration of response was longer, and their progression-free survival was superior
515 compared to those who demonstrated increasing biomarkers prior to therapy. Our study
516 highlights the benefit of including evolving disease as an indication of high-risk disease.

517 Future studies will help shed light on the importance of varying biomarkers in terms of risk
518 stratification and the severity of disease.

519
520 Genomic alterations are critical to better define patients who are truly at risk of
521 progression and who may benefit from more aggressive therapy. In this study, the
522 addition of WGS and single-cell RNA sequencing helped identify participants with high-
523 risk cytogenetics who otherwise would not have been identified by FISH alone. We opted
524 not to include MAPK and DNA repair pathway mutations in analyzing impact on outcomes
525 because we did not have data available on all patients. With additional data, we were able
526 to indeed define a population of high-risk cytogenetics and poor response to therapy who
527 showed the worst outcome.

528
529 Minimal residual disease was performed with two approaches in this protocol: standard
530 FDA-approved NGS on BM samples achieving at least VGPR and very sensitive MALDI-
531 TOF mass spectrometry. MALDI-TOF was assessed on peripheral blood serum, avoiding
532 bone marrow biopsy, and is gaining more and more interest in the field. We showed that
533 MALDI-TOF is a sensitive and accurate assay for monitoring M protein isotype and
534 quantification, with a concordance with SPEP at baseline and a strong prognostic effect
535 after EOT. We showed that MALDI-TOF is superior to IFX with 100% NPV and 83% PPV,
536 similar to previous studies³⁵.

537
538 We performed an integrative study combining WGS and single-cell RNA-sequencing of
539 tumor and immune cells with the IRD study. To identify tumor-specific gene expression
540 differences that associated with IRD treatment response, we compared gene expression
541 in tumor cells at baseline from progressor and non-progressor patients who
542 received IRD. We observed significantly higher levels of MHC class I genes in tumor cells
543 from non-progressor patients compared to progressors. We further validated this finding
544 using data from an external study on MM patients treated with a different proteasome
545 inhibitor (Bortezomib), suggesting a broader link between MHC-I levels and response to
546 proteasome inhibition. To further explore the immune system's involvement, we
547 analyzed cytotoxic CD8+ T cells, which recognize and eliminate cells presenting specific
548 antigens on their surface via MHC-I molecule. We compared the clonal expansion of two
549 T cell subsets, granzyme K (GZMK)+ and granzyme B (GZMB)+, and found that
550 progressors exhibited greater clonal expansion in the GZMK+ compartment compared to
551 non-progressors, suggesting a potentially ineffective immune response. We have
552 previously shown that the GZMK+ compartment is the major source of expression of PD-
553 1, a key T cell exhaustion marker²⁰. Additionally, progressors showed a reduced
554 proportion of the GZMB+ phenotype within their clonally expanded T cells,
555 suggesting their clonally expanded T cells have a less mature cytotoxic profile compared
556 to those of non-progressors. We next analyzed functional differences in T cells between
557 progressors and non-progressors. Gene expression patterns revealed higher expression
558 of genes related to cytotoxicity and activation in the non-progressors' clonally expanded
559 GZMB+ T cells compared to those of the progressors. Clonally expanded GZMB+ T
560 cells from progressors showed increased expression of genes associated with apoptosis
561 and suppression of cytotoxic responses, alongside markers of maturation. This suggests
562 a more complex picture of functionality in these T cells from progressors. Our findings

563 suggest that immune dysfunction related to changes in tumor intrinsic antigen
564 presentation at baseline may contribute to suboptimal responses in proteasome inhibitor
565 therapy.

566
567 Our study has several limitations including the non-randomized nature of the trial without
568 a control arm and the potential selection bias in any single-center experience. Several
569 questions remain, including optimal timing of therapy in HR-SMM, duration of therapy,
570 treatment modality (combinations, immunotherapy), and response adaptive approaches.
571 The limited size of the scRNAseq sub-cohort and lack of functional validation limit the
572 conclusiveness of the findings and require further validation in larger, independent
573 cohorts.

574
575 In conclusion, this is the first trial studying an all-oral triplet combination of ixazomib,
576 lenalidomide, and dexamethasone in HR-SMM, demonstrating substantial efficacy and
577 identifying several factors critical in the outcome of patients: depth of response, evolving
578 pattern, MRD negativity and high risk 20/2/20. Future studies using quadruplet therapy or
579 immunotherapy may alter these conclusions.

580

581 **Methods**

582
583 The research study was approved by the Dana-Farber/Harvard Cancer Center
584 institutional review board (protocol number DFCI 16-313) and complied with all relevant
585 ethical and legal regulations. All participants gave written informed consent. The
586 clinicaltrials.gov registration number is NCT02916771. Individual deidentified participant
587 sequencing and FISH data will be shared.

588

589 Eligibility Criteria

590
591 Patients enrolled on the study met eligibility for high-risk SMM based on criteria by
592 Rajkumar²⁴ as follows: bone marrow plasmacytosis $\geq 10\%$ and $\leq 60\%$ and any one or
593 more of the following: serum M protein ≥ 3 g/dL, IgA isotype, immune paresis with
594 reduction of 2 uninvolved immunoglobulins, serum involved/uninvolved ratio of ≥ 8 but
595 ≤ 100 , bone marrow plasmacytosis 50-60%, abnormal plasma cell immunophenotype,
596 high-risk FISH defined as t(4;14), del 17p or 1q gain, increased circulating plasma cells,
597 MRI with diffuse abnormalities or 1 focal lesion, PET/CT with one focal lesion with
598 increased uptake without underlying osteolytic bone destruction and urine monoclonal
599 light chain excretion ≥ 500 mg/24 hours. Patients with evidence of SLiM-CRAB criteria
600 were excluded (bone marrow plasmacytosis $> 60\%$, light chain ratio > 100)³⁶. Patients
601 were required to have an ECOG performance status of ≤ 2 and adequate hematologic and
602 organ function prior to enrollment. A creatinine clearance of ≥ 30 mL/min was required.

603

604 Treatment Regimen

605
606 Patients were treated on an outpatient basis with 9 cycles of induction therapy consisting
607 of ixazomib 4mg given orally on days 1, 8, and 15, in combination with lenalidomide 25mg
608 administered orally on days 1 through 21 and dexamethasone 40mg administered orally

609 on days 1, 8, 15, and 22 of a 28-day cycle. The induction phase was followed by
610 maintenance therapy, consisting of ixazomib 4mg on days 1, 8, and 15 and lenalidomide
611 15mg on days 1-21 without dexamethasone for another 15 cycles. Treatment duration
612 was a total of 24 cycles (2 years).

613

614 Objectives and End Points

615

616 The primary objective was to determine the proportion of patients with HR-SMM who are
617 progression-free 2 years after receiving trial therapy. Progression for the primary endpoint
618 was defined as the development of end organ damage per SLiM-CRAB criteria.
619 Secondary objectives included response rates, duration of response, progression-free
620 survival, safety of the combination therapy, and minimal residual disease (MRD)
621 negativity. Mass spectrometry analysis was also performed to correlate with IMWG
622 response and MRD status.

623

624 Minimal Residual Disease Assessment and Mass Spectrometry

625

626 MRD was assessed by the next-generation sequencing (NGS) ClonoSEQ® assay
627 (Adaptive Biotechnologies, Seattle, WA, USA) on bone marrow samples from patients
628 who achieved at least a very good partial response (VGPR) at cycle 9 (C9) or later. When
629 BM was available, a second MRD assessment was performed to confirm the MRD result.
630 Quality control (QC) of NGS results was performed as previously described³⁷.

631

632 Minimal residual disease by next-generation sequencing was evaluable in 25 patients
633 who achieved at least a VGPR. Baseline pre-treatment bone marrow samples were
634 available for 22/25 patients and were analyzed for the identification of the VDJ molecular
635 marker by the Adaptive MRD assay. Twenty out of 22 (91%) baseline samples passed
636 the QC analysis, and the molecular marker was identified in 18/22 patients (82%). For
637 MRD analysis of these 18 patients, bone marrow samples that were available from end
638 of induction (C9) and from the end of treatment (EOT) were used for sequencing. Three
639 of the 18 patients did not have any sample available for MRD analysis and one sample
640 had indeterminate results at limits of detection, 13 patients had MRD testing at the end of
641 induction (C9), 10 at EOT, and 8 individuals had an assessment at both timepoints for an
642 overall total of 23 samples tested for MRD.

643

644 Residual disease after therapy was also assessed by matrix-assisted laser desorption
645 ionization-time of flight (MALDI-TOF) mass spectrometry to quantify M proteins (Binding
646 Site Group, Birmingham, UK), and Optilite free light-chain assay to quantify IgG, IgA, IgM,
647 and serum free light chains. EXENT-iQ software (Binding Site Group, Birmingham, UK)
648 was used for quantitative analysis of detected M proteins. The lower limit of accurate M
649 protein quantification by MALDI-TOF mass spectrometry was 0.015 g/L. Serum (500 µL)
650 was tested using the EXENT system and immunoglobulin (Ig) isotype assay³⁸. The unique
651 mass/charge (m/z) (+/- 5) of a monoclonal light chain and the isotype were defined at
652 baseline and tracked in each patient's samples after therapy at the end of induction (C9)
653 and when available during maintenance (2-3 months after C9) and at end of treatment
654 (EOT). MALDI-TOF was performed at baseline before treatment in 48 patients out of 55.

655 Seven out of 55 patients were excluded due to sample unavailability ($n = 5/7$) and light
656 chain-only disease at baseline ($n = 2$ out of 55), defined as having a negative SPEP and
657 serum immunofixation (IFX) result in the setting of SMM (**Suppl Figure S2**). We assessed
658 the concordance between Isotype by MALDI-TOF and SPEP-IFX and the correlation
659 between quantified M protein at baseline with the two methods using Pearson correlation.
660 The concordance between NGS MRD results and residual disease by MALDI-TOF was
661 also assessed by comparing the presence of residual M protein >0.015 g/L (limit of
662 detection)³⁹ and positivity at 10^{-5} by NGS. Concordance between MS by MALDI-TOF, IFX,
663 and NGS in BM was assessed using Cohen's kappa (κ) statistic, with κ value
664 interpretation per Landis and Koch⁴⁰.

665 666 DNA isolation and library construction

667 Genomic DNA isolation was carried out using the Monarch Genomic DNA Purification Kit
668 (New England Biolabs), with tumor (PCs) and normal (PBMCs) yields quantified by Qubit
669 3.0 fluorometer (Thermo Fisher Scientific). 50-100ng was taken forward for DNA
670 sequencing library preparation using the NEBNext Ultra II FS DNA Library Prep kit (New
671 England Biolabs) with unique dual index adapters (NEBNext Multiplex Oligos) according
672 to manufacturers' instructions. Final library fragment sizes were assessed using the
673 BioAnalyzer 2100 (Agilent Technologies), and yields were quantified by Qubit 3.0
674 fluorometer (Thermo Fisher Scientific) and qPCR (KAPA Library Quantification Kit).

675 676 Whole genome sequencing (WGS) and genomic data analysis

677 WGS was available for 17 patients. Final sample libraries were normalized and pooled
678 before WGS was performed on Illumina NovaSeq 6000 S4 flow cells, 300 cycles 2x150bp
679 paired-end reads, at the Genomics Platform of the Broad Institute of MIT and Harvard.
680 WGS analysis was performed on an in-house cloud-based HPC system for copy-number
681 and structural variant analyses, as previously described⁴¹. Sequencing reads were
682 aligned to the GRCh38 reference genome with the bwa mem v0.7.7 algorithm⁴², duplicate
683 reads were marked with MarkDuplicates from picard v1.457, indels were realigned with
684 GATK 3.4 IndelRealigner, and base qualities were recalibrated with GATKBQSR. WGS
685 analysis was performed with the Cancer Genome Analysis workflow from the Cancer
686 Program at Broad Institute of MIT and Harvard on an in-house cloud-based HPC system.
687 Small indels were called with Strelka2 and were filtered (i) against a panel of normals
688 (PoN), (ii) for potential technical artifacts (oxoG), and (iii) for multiple alignment with
689 BLAT⁴³. After copy-number normalization with AllelicCapSeg, ABSOLUTE solutions were
690 manually reviewed to estimate mutation CCF, purity, and ploidy of tumor samples⁴⁴.
691 Structural variants were detected and filtered as previously described⁴⁵.

692 693 Patient sample processing for scRNA-seq

694 Whole bone marrow aspirates (5-20mLs) were drawn into EDTA preservative tubes and
695 kept at 4°C before being processed within a 6 hours from collection. Bone marrow
696 mononuclear cells were isolated from aspirates using density gradient centrifugation.
697 Briefly, the bone marrow was filtered to remove any clots or bone debris, diluted 1:3 with
698 1X Phosphate-Buffered Saline (PBS), and gently poured above 15mLs of Ficoll-Paque
699 density gradient medium within a SepMate™ PBMC isolation tube (StemCell
700 Technologies, Cat # 85450). After centrifugation at 1200 rcf/g for 15 minutes, PBMCs

701 were poured away from unwanted cells and washed twice with ice-cold 1xPBS prior to
702 plasma cell enrichment. Plasma cells were enriched from the bone marrow samples using
703 CD138 magnetic bead separation using single-column positive selection (Miltenyi Biotec,
704 Cat #130-097-614).

705
706

707 Single-cell RNA/V(D)J library construction and sequencing

708 Sequencing libraries were prepared from BM samples, including 5' scRNA-seq libraries
709 and scBCR-seq and scTCR-seq libraries. After MACS enrichment, all CD138+ and
710 CD138- cells were centrifuged at 300 rcf/g for 5 mins and washed twice with an ice-cold
711 0.1% Ultrapure Bovine Serum Albumin (BSA)/PBS wash buffer. Subsequently, cells were
712 either subjected to volume reduction or diluted based on cell counts obtained using both
713 a hemocytometer and a Countess automated cell counter (ThermoFisher) and cell
714 mixtures were adjusted to obtain optimal cell densities for achieving maximal cell
715 recovery. Samples, Gel bead-in-EMulsion (GEMs), and partitioning oil were loaded into
716 a Next GEM Chip K microfluidic device and placed in a Chromium Controller instrument
717 for downstream single-cell encapsulation and recovery. All GEM generation/barcoding,
718 post GEM RT clean-up/cDNA amplification and 5' gene expression (GEX) library
719 construction steps were completed using the Chromium Next GEM Single Cell 5' Reagent
720 Kit v2 (Dual Index) and Library Construction Kit, according to the manufacturer's
721 instructions. cDNA generated was also subsequently subjected to V(D)J amplification
722 using Chromium Single Cell Human BCR Amplification Kit and Library Construction Kit
723 for scBCR-seq and Chromium Single Cell Human TCR Amplification Kit and Library
724 Construction Kit for scTCR-seq, according to the manufacturer's instructions. The quality
725 of sample libraries was assessed based on library trace fragment sizes and patterns at
726 numerous points throughout the protocol including cDNA generation, BCR V(D)J pre-
727 amplified cDNA generation, TCR V(D)J pre-amplified cDNA generation, final GEX, final
728 BCR and final TCR construction steps using a High-Sensitivity DNA Analysis Kit and the
729 Bioanalyzer 2100 instrument (Agilent Technologies). Final GEX, BCR and TCR library
730 quantification was performed using Quant-iT Picogreen dsDNA Assay Kit (Invitrogen)
731 before preparing single pools for sequencing. Pooled libraries were sequenced on
732 NovaSeq S4 flow cells at the Genomics Platform of the Broad Institute of MIT and Harvard
733 (Cambridge, MA).

734
735

736 Single-cell RNA/V(D)J data processing

737 CD138+ scRNA-seq was available for 13 patients, CD138- scRNA-seq was available for
738 20 patients and 12 patients had paired CD138+ and CD138- scRNA-seq. Paired WGS
739 and CD138+ RNA sequencing was available for 10 patients. 20 patients had either
740 scRNA-seq or WGS performed on their tumor samples.

741 CellRanger mkfastq (v5.0.1) was used to generate FASTQ files⁴⁶. Gene expression
742 matrices were generated by CellRanger count (v6.0.1) with the genome reference
743 (refdata-gex-GRCh38-2020-A) provided by 10X Genomics⁴⁶. To remove ambient RNA,
744 CellBender (v0.2.0) was run on the gene expression matrices with the target false positive
745 rate cutoff of 0.01. Poor quality cells with >15% mitochondrial gene expression, either
746 <200 detected genes, >5,000 detected genes, <400 UMIs, or >50,000 UMIs were filtered

747 out. Three doublet tools, Scrublet (v0.2.3), scDbiFinder (v1.8.0), and scds (1.10.0) were
748 used to calculate multiplet scores⁴⁷⁻⁴⁹. CellRanger vdj (v6.0.1) was used on FASTQ files
749 with the VDJ reference file (refdata-cellranger-vdj-GRCh38-alts-ensembl-5.0.0)⁴⁶.

750

751 Malignant plasma cell identification

752 Plasma cells were first identified based on expressing key lineage markers, such as
753 *SDC1* (encoding CD138), *CD38*, *XBP1*, *PRDM1*, *IRF4*, and *TNFRSF17* (encoding
754 BCMA). Cell barcodes that were determined to correspond to plasma cells were
755 considered for downstream analysis. Tumor cells were identified on the basis of belonging
756 to the largest expanded BCR clone and clustering separately from normal plasma cells.
757 For all clones, the isotype of the malignant clone matched that detected clinically via IFX.
758 We annotated 50,591 of patient cells as tumor, and the rest (n=1876) as healthy plasma
759 cells based on our tumor cell annotation protocol. The median number of tumor cells per
760 patient was 2,148 .

761

762 Single-cell TCR sequencing data processing and analysis

763 We performed single-cell TCR sequencing on CD138- samples with available single-cell
764 RNA sequencing data (n=9). Complementary DNA generated from barcoded CD138-
765 immune cells using Chromium Single Cell 5' Gene Expression and V(D)J enrichment kits
766 by 10X Genomics was subjected to V(D)J enrichment and library preparation and
767 sequenced on a NovaSeq 6000 instrument at the Genomics Platform of the Broad
768 Institute of MIT & Harvard.

769 CellRanger v5.0.1 was used to extract FASTQ files and produce clonotype matrices⁵⁰ .
770 When multiple alignments were called for a single chain, the alignment with the most
771 UMIs was selected, and when multiple chains were called for a single cell barcode, the
772 top two chains in terms of UMI counts were selected.

773 Clone size assignment:

774 To categorize TCR clones based on its size or its abundance within a sample, we
775 employed a downsampling approach to account for potential sampling bias. We randomly
776 sampled 100 T cells from each patient sample 100 times. Within each iteration, we
777 calculated the proportion of each unique TCR clone compared to the total T cells sampled.
778 Finally, for each clone, we averaged its proportional abundance across all iterations to
779 obtain a more stable estimate of its size category. Categories were defined as: Rare:
780 $\leq 1\%$, Small: $> 1\%$ and $< 5\%$, Medium: $\geq 5\%$ and $< 10\%$, Large: $\geq 10\%$.

781 Clone-size-category proportion estimation within cell subtypes per patient sample:

782 To estimate the overall proportion of clones belonging to each size category within a cell
783 subtype per patient sample, we again used downsampling. We randomly sampled 100 T
784 cells from each patient cell subtype sample 100 times. In each iteration, we counted the
785 frequency of each clone size category within the downsampled set. Finally, we averaged
786 the frequency of each category across all iterations and these averaged frequencies were
787 then renormalized before plotting. Two-sided p-values were computed by bootstrapping
788 with 1000 iterations.

789

790 Copy number analysis from scRNA sequencing

791 Copy number abnormalities on tumor cells were inferred using Numbat with default
792 parameters (v1.1.0)²². Allelic data was collected from plasma cells and B cells and a panel
793 of 1,200 plasma cells from 11 healthy donors was used as expression reference.

794

795 Differential Expression Analysis

796 Droplets with < 20,000 reads per cell were discarded, and 20,000 reads per cell were
797 downsampled across the entire CD138pos scRNA-seq cohort. To control the influence of
798 individual tumors on the analysis, as well as control for the lower number of non-
799 progressors in this sub-cohort (n=3, compared to 10 progressors), we randomly sampled
800 the same number of tumor cells from progressors and non-progressors (~2100 per group)
801 and balanced the contribution of each individual towards the group (progressors: 210 cells
802 per patient as one progressor patient had fewer than 210 cells (n=72) after downsampling;
803 non-progressors: 700 cells per patient). We repeated this process leaving out the one
804 progressor patient with low number of cells this time considering only 9 progressor
805 patients and 3 non-progressors and once again balancing the contribution of each
806 individual towards the group (progressors n=225, non-progressors n=675 per patient). No
807 difference in results was observed.

808

809 Statistical Analysis

810 The primary outcome was progression-free survival after two years of study treatment.
811 Progression-free was defined as being followed for at least two years from the start of
812 protocol therapy and no confirmed disease progression. The primary endpoint was
813 calculated for both progression to SLIM-CRB criteria as well as biochemical progression.

814

815 For this manuscript, progressive disease was defined as per the IMWG uniform
816 response criteria for MM with either SLIM-CRAB progression or a rise of 25% in serum
817 or urine M protein or difference between involved and uninvolved FLC levels⁵¹.

818

819 Patients who did not have at least 2 years of follow-up or progressed between the start
820 of treatment and two years after EOT were counted as failed progression-free at 2 years.
821 The study was designed for a 50 vs 70% progression-free rate with 5% and 10% type I
822 and type II errors, respectively. The critical value to reject the null hypothesis of 50% was
823 33 or more of 53 patients and was evaluated using a one-sided exact binomial test.

824

825 We report the primary outcome and responses to study treatment as proportions with
826 90% exact binomial confidence intervals. Continuous measures are summarized by
827 median and range, and categorical variables are summarized as proportions.

828 Categorical variables were tested for association with continuous and other categorical
829 variables using Wilcoxon rank-sum (or Kruskal-Wallis for three or more groups) or
830 Fisher's exact tests, respectively. Time-to-event endpoints are estimated using the
831 method of Kaplan and Meier with 95% confidence intervals calculated using
832 Greenwood's method to estimate variance. Median follow-up is calculated using the
833 reverse Kaplan-Meier method. Statistical analyses were performed using R version
834 4.1.2 (2021-11-01).

835
836
837
838
839
840
841
842
843
844
845
846
847
848
849
850
851
852
853
854
855
856
857
858
859
860
861
862
863
864
865
866
867
868
869
870
871
872
873
874
875
876
877
878
879
880

Acknowledgments

The authors would like to thank the patients and their families for participating in this study.

Anna V. Justis, PhD, a medical writer employed by Dana-Farber Cancer Institute, edited this manuscript under the direction of the authors.

Authorship Contributions

O.N.: Writing-Original Draft, Writing-Review & Editing

M.P.A.: Writing-Original Draft, Investigation, Formal analysis, Visualization, Writing-Review & Editing

R.A.R.: Formal analysis, Visualization, Writing-Review & Editing

M.T: Formal analysis, Visualization, Writing-Review & Editing

S.M.: Writing-Review & Editing

J.A. Writing-Review & Editing, Supervision

L.B.: Investigation, Writing-Review & Editing

A.D. Writing-Review & Editing, Supervision

H.E.: Investigation, Writing-Review & Editing

M.B.: Investigation, Writing-Review & Editing

E.D.L.: Investigation, Writing-Review & Editing

J.P.L.: Writing-Review & Editing

G.B.: Writing-Review & Editing

E.O.: Writing-Review & Editing

T.W.: Writing-Review & Editing

J.T.: Writing-Review & Editing

K.A.: Writing-Review & Editing

P.G.R.: Writing-Review & Editing

G.G.: Writing-Review & Editing

L.T.: Writing-Review & Editing, Supervision

R.S.P.: Writing-Review & Editing, Supervision

I.M.G.: Conceptualization, Resources, Writing-Review & Editing, Supervision, Funding Acquisition

Declaration of Interests

ON: Research support from Takeda and Janssen; Advisory board participation: Bristol Myers Squibb, Janssen, Sanofi, Takeda, GPCR therapeutics. Honorarium: Pfizer

M.P.A: No conflicts of interest exist.

R.A.R.: No conflicts of interest exist.

M.T: No conflicts of interest exist.

S.M.: No conflicts of interest exist.

J.B.A. No conflicts of interest exist.

881 L.B.: No conflicts of interest exist.
882 A.K.D. No conflicts of interest exist.
883 H.E.: No conflicts of interest exist.
884 M.B.: Consultancy with Janssen, BMS, Takeda, Epizyme, Karyopharm, Menarini
885 Biosystems, and Adaptive.
886 E.D.L.: No conflicts of interest exist.
887 J.P.L.: No conflicts of interest exist.
888 G.B.: Consultancy: Prothena
889 E.O.: Advisory Board/Honoraria: Janssen, BMS, Sanofi, Pfizer, Exact Consulting—
890 Takeda Steering Committee: Natera
891 T.W.: No conflicts of interest exist.
892 J.T.: No conflicts of interest exist.
893 K.A.: Consultant: AstraZeneca, Janssen, Pfizer, Board/ Stock Options: Dynamic Cell
894 Therapies, C4 Therapeutics, Next RNA, Oncopep, Starton, Window
895 G.G.: No conflicts of interest exist.
896 L.T.: No conflicts of interest exist.
897 P.G.R.: Advisory Boards/Consulting: Celgene/BMS, GSK, Karyopharm, Oncopeptides,
898 Regeneron, Sanofi, Takeda. Research Grants: Oncopeptides, Karyopharm
899 R.S.P.: Co-founder, equity holder, and consultant on pre-seed stage startup.
900 I.M.G.: Consulting/Advisory role: AbbVie, Adaptive, Amgen, Aptitude Health, Bristol
901 Myers Squibb, GlaxoSmithKline, Huron Consulting, Janssen, Menarini Silicon
902 Biosystems, Oncopeptides, Pfizer, Sanofi, Sognef, Takeda, The Binding Site, and
903 Window Therapeutics; Speaker fees: Vor Biopharma, Veeva Systems, Inc.; I.M.G.'s
904 spouse is CMO and an equity holder of Disc Medicine.

905

906 **Inclusion and Ethics**

907 One or more of the authors of this paper self-identifies as an underrepresented ethnic
908 and/or gender minority in science. One or more of the authors of this paper self-identifies
909 as a member of the LGBTQIA+ community. We support inclusive, diverse and equitable
910 conduct of research.

911

912 **Data availability**

913 Single-cell RNA and TCR-sequencing raw data generated for this study will be deposited
914 in dbGaP (study site pending). Gene expression matrices can be accessed on Mendeley:
915 [https://data.mendeley.com/preview/z56k3y8cdg?a=6945f72a-b190-4fb1-b0fe-](https://data.mendeley.com/preview/z56k3y8cdg?a=6945f72a-b190-4fb1-b0fe-31c12a70a0d4)
916 [31c12a70a0d4](https://data.mendeley.com/preview/z56k3y8cdg?a=6945f72a-b190-4fb1-b0fe-31c12a70a0d4) (reserved DOI:10.17632/z56k3y8cdg.1)

917

918

919 **Code Availability**

920 This paper does not report original code.

921

922 **Figure Legends**

923

924 **Figure 1. A)** Consort Diagram **B)** Primary events such as translocations and
925 hyperdiploidy and secondary events such as copy number alterations identified by
926 FISH, WGS, and scRNA-seq along with response to therapy. WGS = Whole genome
927 sequencing, scRNA = Single-cell RNA sequencing. scRNA-seq revealed a more complex
928 aberration in one case (HRD with trisomies of chromosomes 5, 9, 11, 15, 19, and 21) compared
929 to whole-genome sequencing (WGS) which only detected trisomies on chromosomes 9 and 15.
930 This explains the apparent discrepancy between WGS finding "no primary event" and scRNA-
931 seq identifying HRD (homologous recombination deficiency) in that case. ND=Not determined,
932 CR=Complete response, VGPR=Very good partial response, PR=Partial response, MR=Minimal
933 response, SD=Stable disease.

934

935 **Figure 2. Swimmer's plot of responses deepening over time.** Each lane represents
936 one participant.

937

938 **Figure 3. Progression-free and overall survival.** Progression defined by **A)**
939 Biochemical progression or **B)** SLiM CRAB criteria **C)** Overall survival. NR = not
940 reached **D)** Kaplan-Meier curve of response duration stratified by 20/2/20 risk groups.
941 **E)** Kaplan-Meier curve of progression stratified by 20/2/20 risk groups. Survival
942 distributions were compared using one-sided log-rank tests.

943

944 **Figure 4. Outcomes stratified by the presence of evolving subtype prior to**
945 **treatment. A)** Overall survival **B)** progression-free survival **C)** time-to-progression and
946 **D)** duration of response. NR = not reached. Survival distributions were compared using
947 one-sided log-rank tests.

948

949 **Figure 5. Kaplan Meier Curve of Progression-Free Survival** based on **A)** Depth of
950 Response of VGPR of greater. VGPR = Very good partial response **B)** depth of
951 response amongst cytogenetically high-risk patients by High-risk patients identified by
952 FISH alone. **C)** by High-risk patients identified by FISH, WGS, or single-cell RNA
953 sequencing. **D)** Kaplan-Meier curve of duration of response stratified by patients who
954 achieved sustained CR. **E)** Kaplan-Meier curve of progression-free-survival stratified by
955 patients who achieved sustained CR. CR = Complete response. Survival distributions
956 were compared using one-sided log-rank tests.

957

958 **Figure 6. Kaplan Meier Curve of Outcomes Based on MRD Status: A).** Overall
959 Survival, **B)** Progression-free survival. Survival distributions were compared using one-
960 sided log-rank tests.

961

962 **Figure 7. Single-cell RNA sequencing of bone marrow CD138+ cells. A)** Time to
963 progression or last follow-up for the subcohort of patients with sequencing data (one
964 patient per row). The type of sequencing data available for individual patients is
965 indicated by green boxes. Patients are grouped by progression status. **B)** Uniform
966 manifold approximation and projection (UMAP) embeddings of patients' and HD's
967 plasma cells that passed quality filtering Cells are colored by the patient from which

968 they originate or patients or HD as a group **C)** UMAP colored by malignancy status
969 (tumor vs normal cells). **D)** UMAP colored by biochemical progression status. **E)**
970 Volcano plot of differential gene expression in progressors and non-progressors. Two-
971 sided p values were computed with Wilcoxon's rank-sum test and corrected using the
972 Benjamini-Hochberg approach. The top 30 genes on either side of the volcano with $q <$
973 0.05 are indicated by stars. **F)** HLA class I expression in patients from the PADIMAC
974 cohort who responded (bortezomib_good) or did not respond (Bortezomib_standard) to
975 bortezomib treatment. Single-cell RNA sequencing of T cells from CD138- samples. **G)**
976 UMAP of T cells **H)** Bar plot visualizing the proportion of clonotypes belonging to each of
977 four clone size categories per patient in BM CD138- samples drawn at BL. For patient's
978 T cell subtype being analyzed, 100 cells were randomly sampled 100 times from non-
979 progressor and progressor patients, and the proportion of expanded (1-rare) clonotypes
980 was compared between the two using bootstrapping with 1000 iterations. The average
981 proportion per clone size category is visualized, and the SD across iterations is depicted
982 in solid-line error bars. **I)** Boxplots, violin plots, and scatterplots comparing the
983 abundance of GZMB+ CD8+ T effector memory (TEM) cells in expanded clones
984 between non-progressors and progressors. Two-sided p values were computed with
985 Wilcoxon's rank-sum test and corrected using the Benjamini-Hochberg approach. **J)**
986 UMAP embedding of progressor and non-progressor patients' BM T cells at BL with
987 matched TCR data. T cells with expanded clones (with a frequency $> 1\%$) are colored
988 by cell type. Cells with rare clonotypes are shown in grey. **K)** Volcano plot of differential
989 gene expression of clonally expanded CD8 TEM in progressors and non-progressors. p
990 values were computed with Wilcoxon's rank-sum test and corrected using the
991 Benjamini-Hochberg approach. Top 30 genes on either side of the volcano with $q < 0.05$
992 are indicated by stars. HD = healthy donors; P = patient; WGS = whole-genome
993 sequencing; HRD = hyperdiploidy
994
995

996 **References**

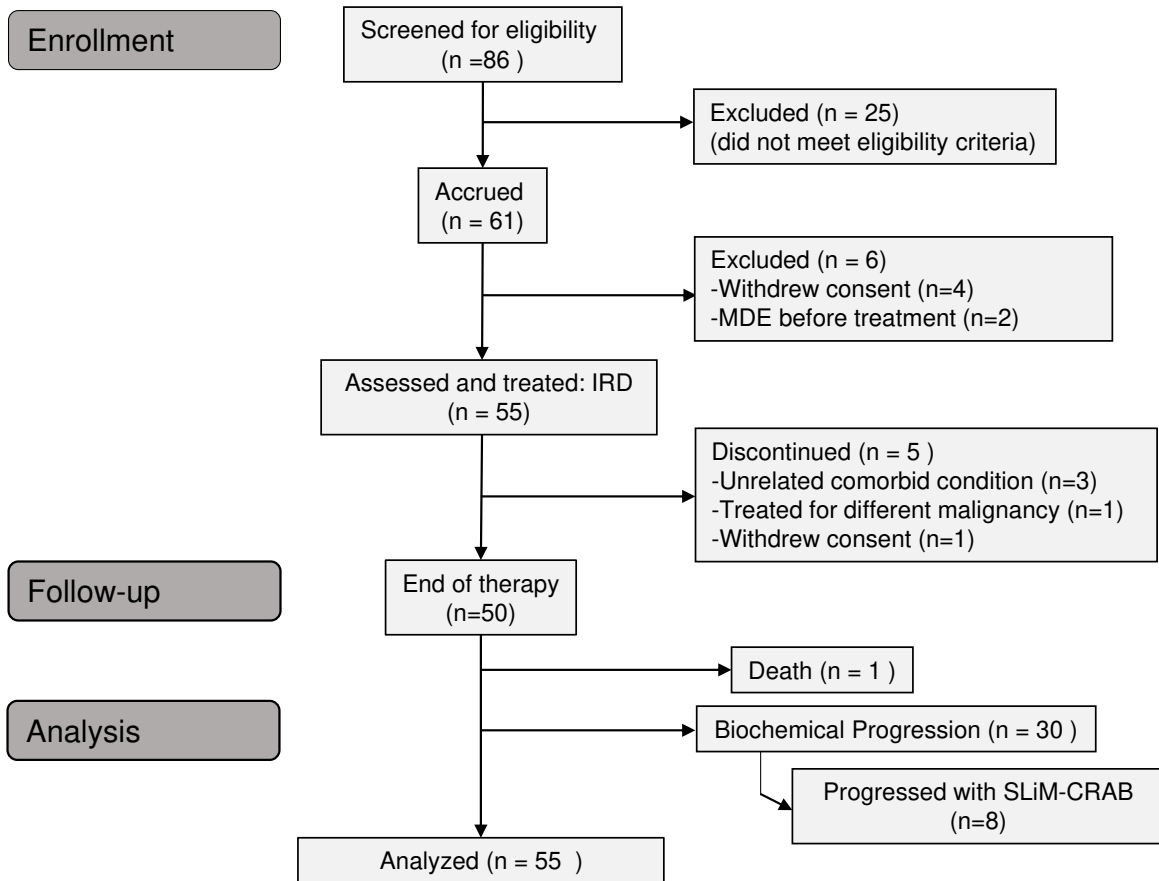
- 997
- 998 1. Kyle RA, Remstein ED, Therneau TM, et al: Clinical course and prognosis of
- 999 smoldering (asymptomatic) multiple myeloma. *N Engl J Med* 356:2582-90, 2007
- 1000 2. Dispenzieri A, Kyle RA, Katzmann JA, et al: Immunoglobulin free light chain
- 1001 ratio is an independent risk factor for progression of smoldering (asymptomatic) multiple
- 1002 myeloma. *Blood* 111:785-9, 2008
- 1003 3. Perez-Persona E, Vidriales MB, Mateo G, et al: New criteria to identify risk of
- 1004 progression in monoclonal gammopathy of uncertain significance and smoldering multiple
- 1005 myeloma based on multiparameter flow cytometry analysis of bone marrow plasma cells. *Blood*
- 1006 110:2586-92, 2007
- 1007 4. Rajkumar SV, Landgren O, Mateos MV: Smoldering multiple myeloma. *Blood*
- 1008 125:3069-75, 2015
- 1009 5. Lakshman A, Rajkumar SV, Buadi FK, et al: Risk stratification of smoldering
- 1010 multiple myeloma incorporating revised IMWG diagnostic criteria. *Blood Cancer J* 8:59, 2018
- 1011 6. Cowan A, Ferrari F, Freeman SS, et al: Personalised progression prediction in
- 1012 patients with monoclonal gammopathy of undetermined significance or smoldering multiple
- 1013 myeloma (PANGEA): a retrospective, multicohort study. *The Lancet Haematology* 10:e203-
- 1014 e212, 2023
- 1015 7. Hill E, Dew A, Morrison C, et al: Assessment of Discordance Among Smoldering
- 1016 Multiple Myeloma Risk Models. *JAMA Oncology* 7:132-134, 2021
- 1017 8. Bustoros M, Sklavenitis-Pistofidis R, Park J, et al: Genomic Profiling of
- 1018 Smoldering Multiple Myeloma Identifies Patients at a High Risk of Disease Progression. *J Clin*
- 1019 *Oncol* 38:2380-2389, 2020
- 1020 9. Bolli N, Maura F, Minvielle S, et al: Genomic patterns of progression in
- 1021 smoldering multiple myeloma. *Nat Commun* 9:3363, 2018
- 1022 10. Misund K, Keane N, Stein CK, et al: MYC dysregulation in the progression of
- 1023 multiple myeloma. *Leukemia* 34:322-326, 2020
- 1024 11. Oben B, Froyen G, Maclachlan KH, et al: Whole-genome sequencing reveals
- 1025 progressive versus stable myeloma precursor conditions as two distinct entities. *Nat Commun*
- 1026 12:1861, 2021
- 1027 12. Boyle EM, Deshpande S, Tytarenko R, et al: The molecular make up of
- 1028 smoldering myeloma highlights the evolutionary pathways leading to multiple myeloma. *Nat*
- 1029 *Commun* 12:293, 2021
- 1030 13. Mateos MV, Hernandez MT, Giraldo P, et al: Lenalidomide plus dexamethasone
- 1031 for high-risk smoldering multiple myeloma. *N Engl J Med* 369:438-47, 2013
- 1032 14. Lonial S, Jacobus S, Fonseca R, et al: Randomized Trial of Lenalidomide Versus
- 1033 Observation in Smoldering Multiple Myeloma. *J Clin Oncol* 38:1126-1137, 2020
- 1034 15. Goodman AM, Kim MS, Prasad V: Persistent challenges with treating multiple
- 1035 myeloma early. *Blood* 137:456-458, 2021
- 1036 16. Avet-Loiseau H, Bahlis NJ: Smoldering Multiple Myeloma : Taking the narrow
- 1037 over the wide path? *Blood*, 2024
- 1038 17. Ghobrial IM, Gormley N, Kumar SK, et al: Round Table Discussion on Optimal
- 1039 Clinical Trial Design in Precursor Multiple Myeloma. *Blood Cancer Discovery:OF1-OF7*, 2024
- 1040 18. Mateos MV LJ, Rodrigues-Otero P, et al. : Curative Strategy (GEM-CESAR) for
- 1041 High-Risk Smoldering Myeloma (SMM): Carfilzomib, Lenalidomide and Dexamethasone (KRd)

- 1042 As Induction Followed By HDT-ASCT, Consolidation with Krd and Maintenance with Rd.
1043 Blood 134:781, 2019
- 1044 19. Kazandjian D, Hill E, Dew A, et al: Carfilzomib, Lenalidomide, and
1045 Dexamethasone Followed by Lenalidomide Maintenance for Prevention of Symptomatic
1046 Multiple Myeloma in Patients With High-risk Smoldering Myeloma: A Phase 2 Nonrandomized
1047 Controlled Trial. *JAMA Oncol* 7:1678-1685, 2021
- 1048 20. Sklavenitis-Pistofidis R, Aranha MP, Redd RA, et al: Immune biomarkers of
1049 response to immunotherapy in patients with high-risk smoldering myeloma. *Cancer Cell*
1050 40:1358-1373.e8, 2022
- 1051 21. Kumar SK, Alsina M, Laplant B, et al: Fixed Duration Therapy with
1052 Daratumumab, Carfilzomib, Lenalidomide and Dexamethasone for High Risk Smoldering
1053 Multiple Myeloma-Results of the Ascent Trial. *Blood* 140:1830-1832, 2022
- 1054 22. Gao T, Soldatov R, Sarkar H, et al: Haplotype-aware analysis of somatic copy
1055 number variations from single-cell transcriptomes. *Nat Biotechnol* 41:417-426, 2023
- 1056 23. Durie BG, Harousseau JL, Miguel JS, et al: International uniform response
1057 criteria for multiple myeloma. *Leukemia* 20:1467-73, 2006
- 1058 24. Rajkumar SV, Dimopoulos MA, Palumbo A, et al: International Myeloma
1059 Working Group updated criteria for the diagnosis of multiple myeloma. *Lancet Oncol* 15:e538-
1060 48, 2014
- 1061 25. Rajkumar SV: Updated Diagnostic Criteria and Staging System for Multiple
1062 Myeloma. *Am Soc Clin Oncol Educ Book* 35:e418-23, 2016
- 1063 26. Lonial S, Jacobus SJ, Weiss M, et al: E3A06: Randomized phase III trial of
1064 lenalidomide versus observation alone in patients with asymptomatic high-risk smoldering
1065 multiple myeloma. *Journal of Clinical Oncology* 37:8001-8001, 2019
- 1066 27. Munshi NC, Avet-Loiseau H, Anderson KC, et al: A large meta-analysis
1067 establishes the role of MRD negativity in long-term survival outcomes in patients with multiple
1068 myeloma. *Blood Advances* 4:5988-5999, 2020
- 1069 28. Daniele P, Mamolo C, Cappelleri JC, et al: Response rates and minimal residual
1070 disease outcomes as potential surrogates for progression-free survival in newly diagnosed
1071 multiple myeloma. *PLoS One* 17:e0267979, 2022
- 1072 29. Gulla A, Morelli E, Samur MK, et al: Bortezomib Induces Anti-Multiple
1073 Myeloma Immune Response Mediated by cGAS/STING Pathway Activation. *Blood Cancer*
1074 *Discovery* 2:468-483, 2021
- 1075 30. Schnell S, Démollière C, van den Berk P, et al: Gimap4 accelerates T-cell death.
1076 *Blood* 108:591-599, 2006
- 1077 31. Tang J, Jia X, Li J, et al: Themis suppresses the effector function of CD8+ T cells
1078 in acute viral infection. *Cellular & Molecular Immunology* 20:512-524, 2023
- 1079 32. Facon T, Venner CP, Bahlis NJ, et al: Oral ixazomib, lenalidomide, and
1080 dexamethasone for transplant-ineligible patients with newly diagnosed multiple myeloma. *Blood*
1081 137:3616-3628, 2021
- 1082 33. Moreau P, Masszi T, Grzasko N, et al: Oral Ixazomib, Lenalidomide, and
1083 Dexamethasone for Multiple Myeloma. *New England Journal of Medicine* 374:1621-1634, 2016
- 1084 34. Ghobrial IM, Gormley N, Kumar SK, et al: Round Table Discussion on Optimal
1085 Clinical Trial Design in Precursor Multiple Myeloma. *Blood Cancer Discovery:OF1-OF7*, 2024
- 1086 35. Puig N, Contreras MT, Agulló C, et al: Mass spectrometry vs immunofixation for
1087 treatment monitoring in multiple myeloma. *Blood Adv* 6:3234-3239, 2022

- 1088 36. Wu V, Moshier E, Leng S, et al: Risk stratification of smoldering multiple
1089 myeloma: predictive value of free light chains and group-based trajectory modeling. *Blood Adv*
1090 2:1470-1479, 2018
- 1091 37. Perrot A, Lauwers-Cances V, Corre J, et al: Minimal residual disease negativity
1092 using deep sequencing is a major prognostic factor in multiple myeloma. *Blood* 132:2456-2464,
1093 2018
- 1094 38. El-Khoury H, Lee DJ, Alberge JB, et al: Prevalence of monoclonal gammopathies
1095 and clinical outcomes in a high-risk US population screened by mass spectrometry: a multicentre
1096 cohort study. *Lancet Haematol*, 2022
- 1097 39. Sakrikar D, Marrot N, North S, et al: Multi-Site Verification of the Automated
1098 EXENT(R) MALDI-TOF-MS System and Immunoglobulin Isotypes Assay for the Identification
1099 and Quantification of Monoclonal Immunoglobulins, 2021 AACC Annual Scientific Meeting,
1100 2021
- 1101 40. Landis JR, Koch GG: The measurement of observer agreement for categorical
1102 data. *Biometrics* 33:159-74, 1977
- 1103 41. Dutta AK, Alberge JB, Lightbody ED, et al: MinimuMM-seq: Genome
1104 Sequencing of Circulating Tumor Cells for Minimally Invasive Molecular Characterization of
1105 Multiple Myeloma Pathology. *Cancer Discov* 13:348-363, 2023
- 1106 42. Li H: Aligning sequence reads, clone sequences and assembly contigs with BWA-
1107 MEM. *arXiv preprint arXiv:1303.3997*, 2013
- 1108 43. Kim S, Scheffler K, Halpern AL, et al: Strelka2: fast and accurate calling of
1109 germline and somatic variants. *Nat Methods* 15:591-594, 2018
- 1110 44. Carter SL, Cibulskis K, Helman E, et al: Absolute quantification of somatic DNA
1111 alterations in human cancer. *Nat Biotechnol* 30:413-21, 2012
- 1112 45. Morton LM, Karyadi DM, Stewart C, et al: Radiation-related genomic profile of
1113 papillary thyroid carcinoma after the Chernobyl accident. *Science* 372, 2021
- 1114 46. Zheng GX, Terry JM, Belgrader P, et al: Massively parallel digital transcriptional
1115 profiling of single cells. *Nat Commun* 8:14049, 2017
- 1116 47. Wolock SL, Lopez R, Klein AM: Scrublet: Computational Identification of Cell
1117 Doublets in Single-Cell Transcriptomic Data. *Cell Syst* 8:281-291.e9, 2019
- 1118 48. Bais AS, Kostka D: scds: computational annotation of doublets in single-cell
1119 RNA sequencing data. *Bioinformatics* 36:1150-1158, 2020
- 1120 49. Germain PL, Lun A, Garcia Meixide C, et al: Doublet identification in single-cell
1121 sequencing data using scDblFinder. *F1000Res* 10:979, 2021
- 1122 50. Zheng GXY, Terry JM, Belgrader P, et al: Massively parallel digital
1123 transcriptional profiling of single cells. *Nature Communications* 8:14049, 2017
- 1124 51. Kumar S, Paiva B, Anderson KC, et al: International Myeloma Working Group
1125 consensus criteria for response and minimal residual disease assessment in multiple myeloma.
1126 *Lancet Oncol* 17:e328-e346, 2016
- 1127

Figure 1

A



B

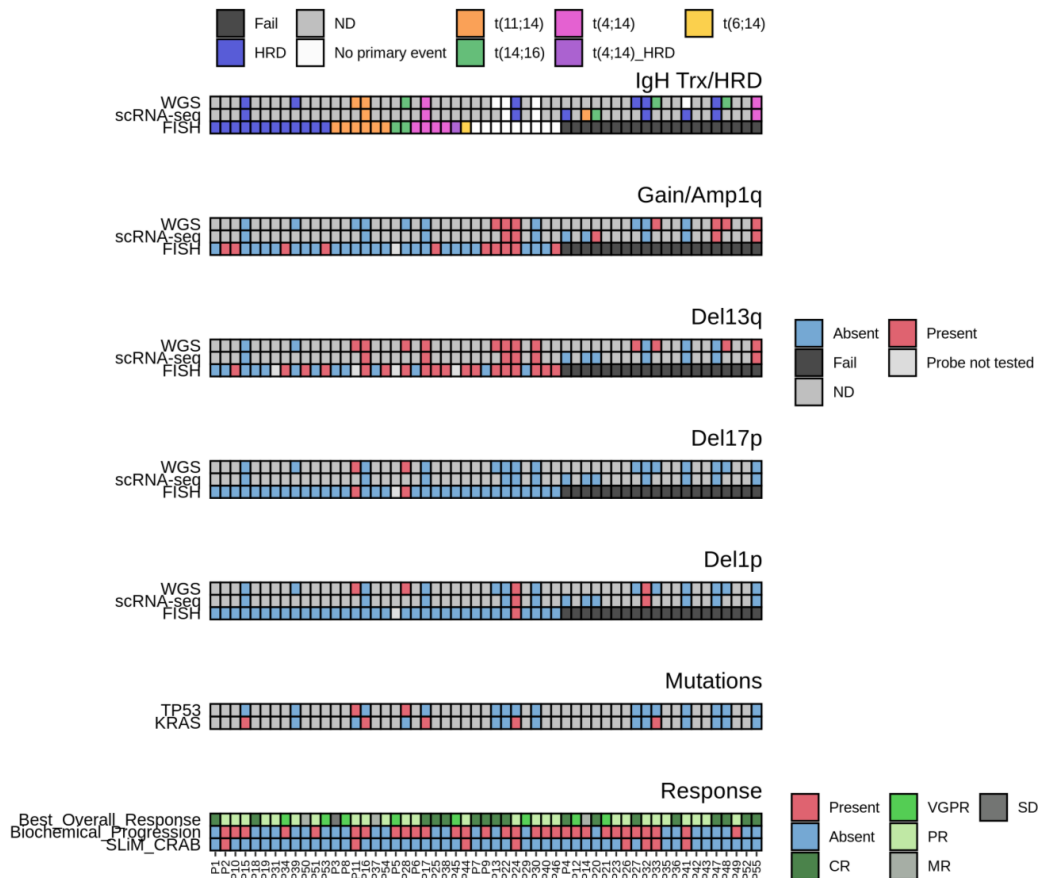


Figure 2

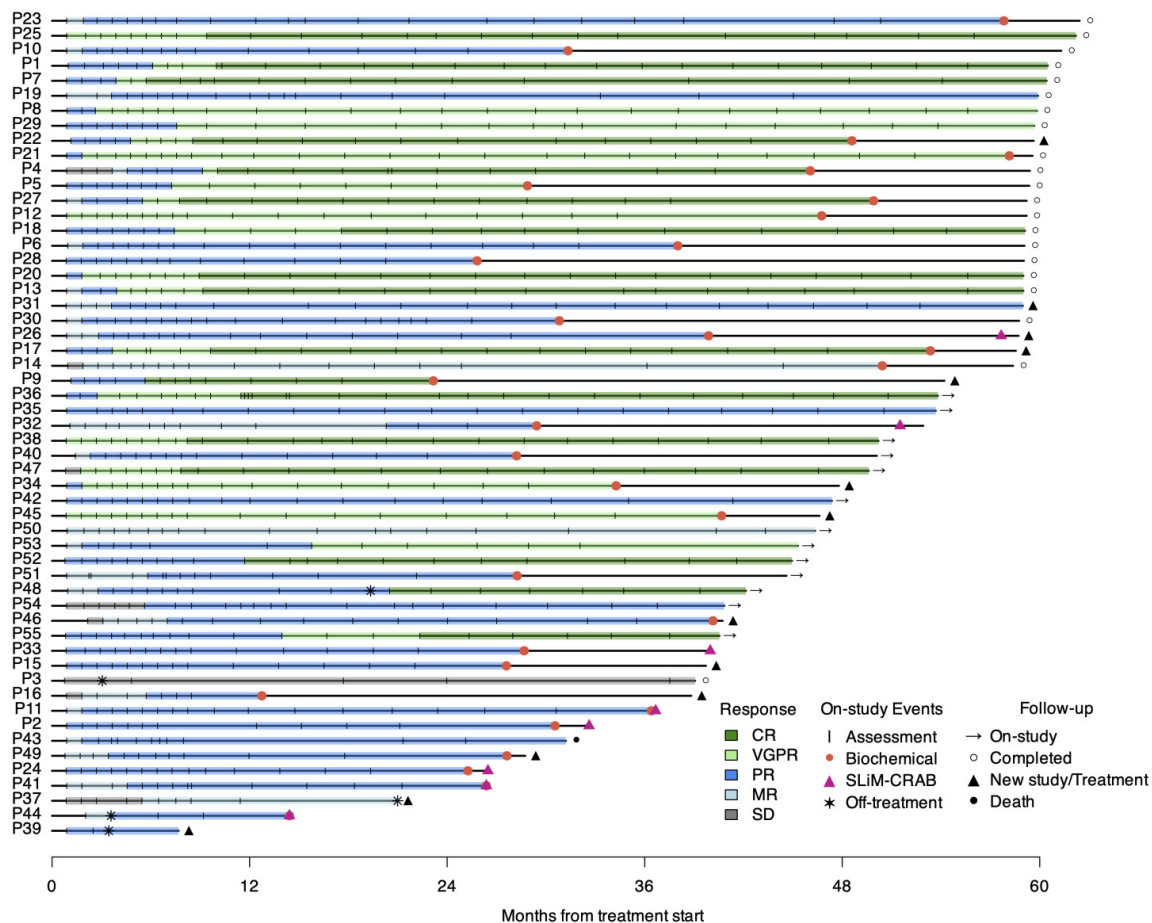


Figure 3

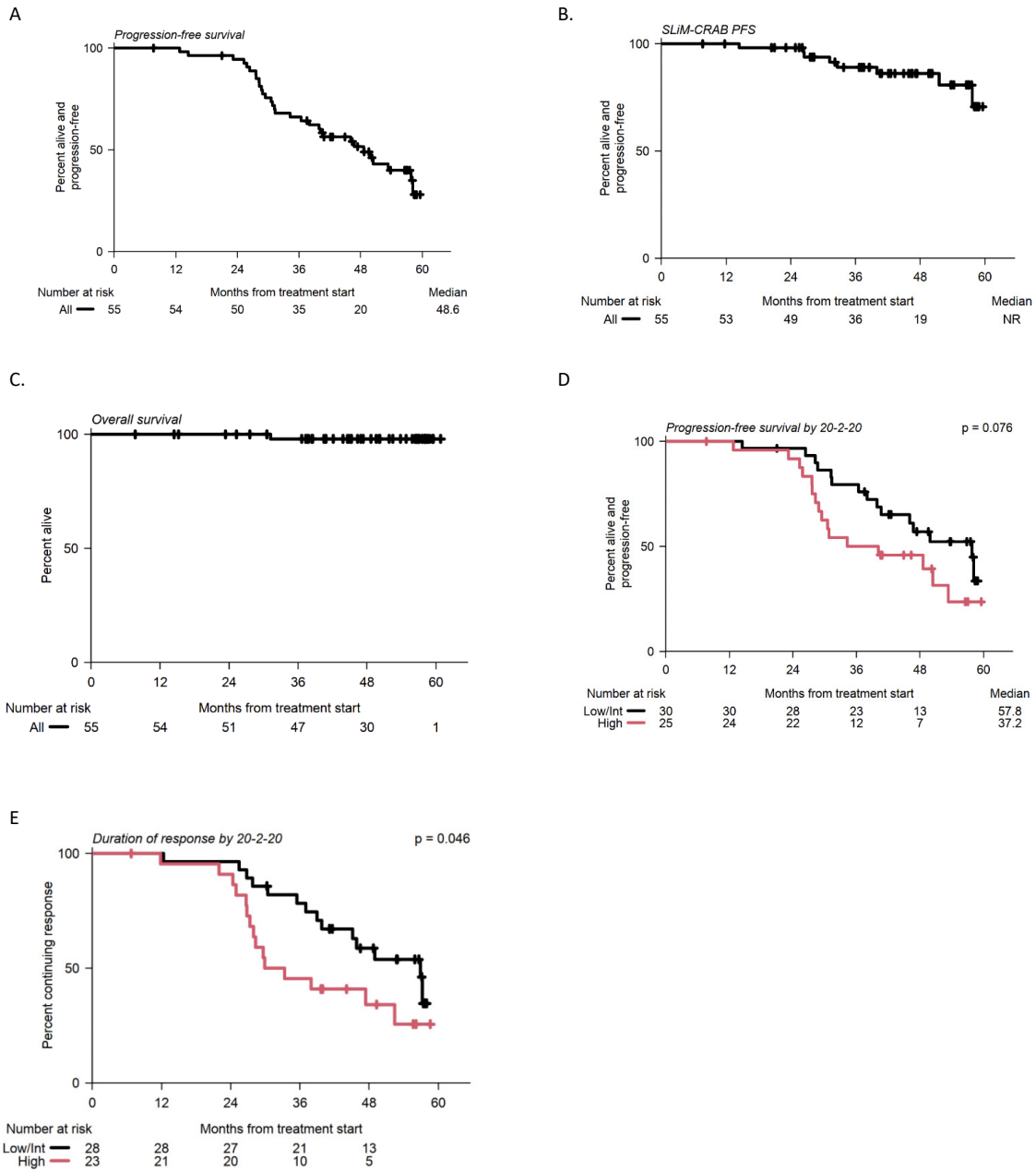


Figure 4

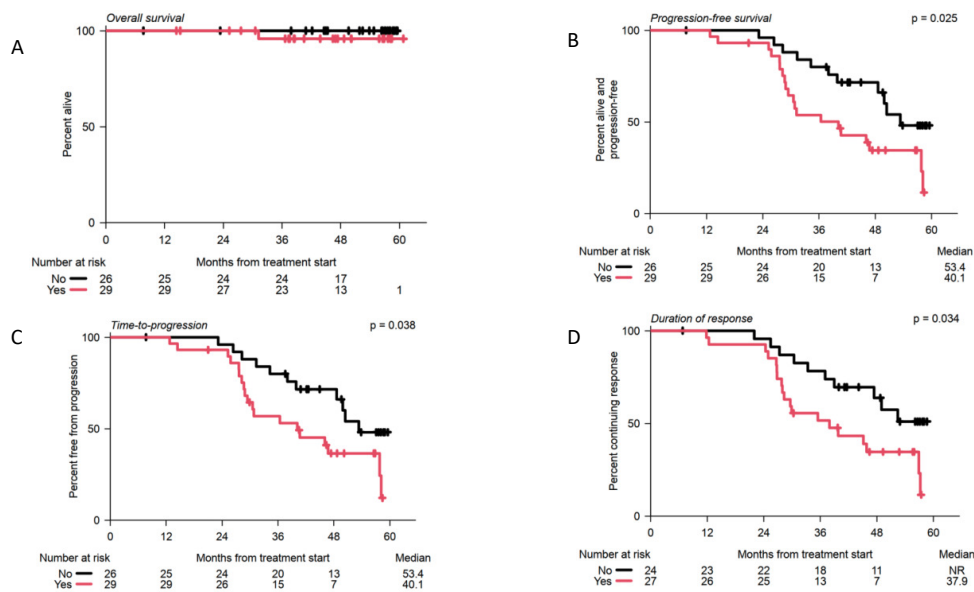


Figure 5

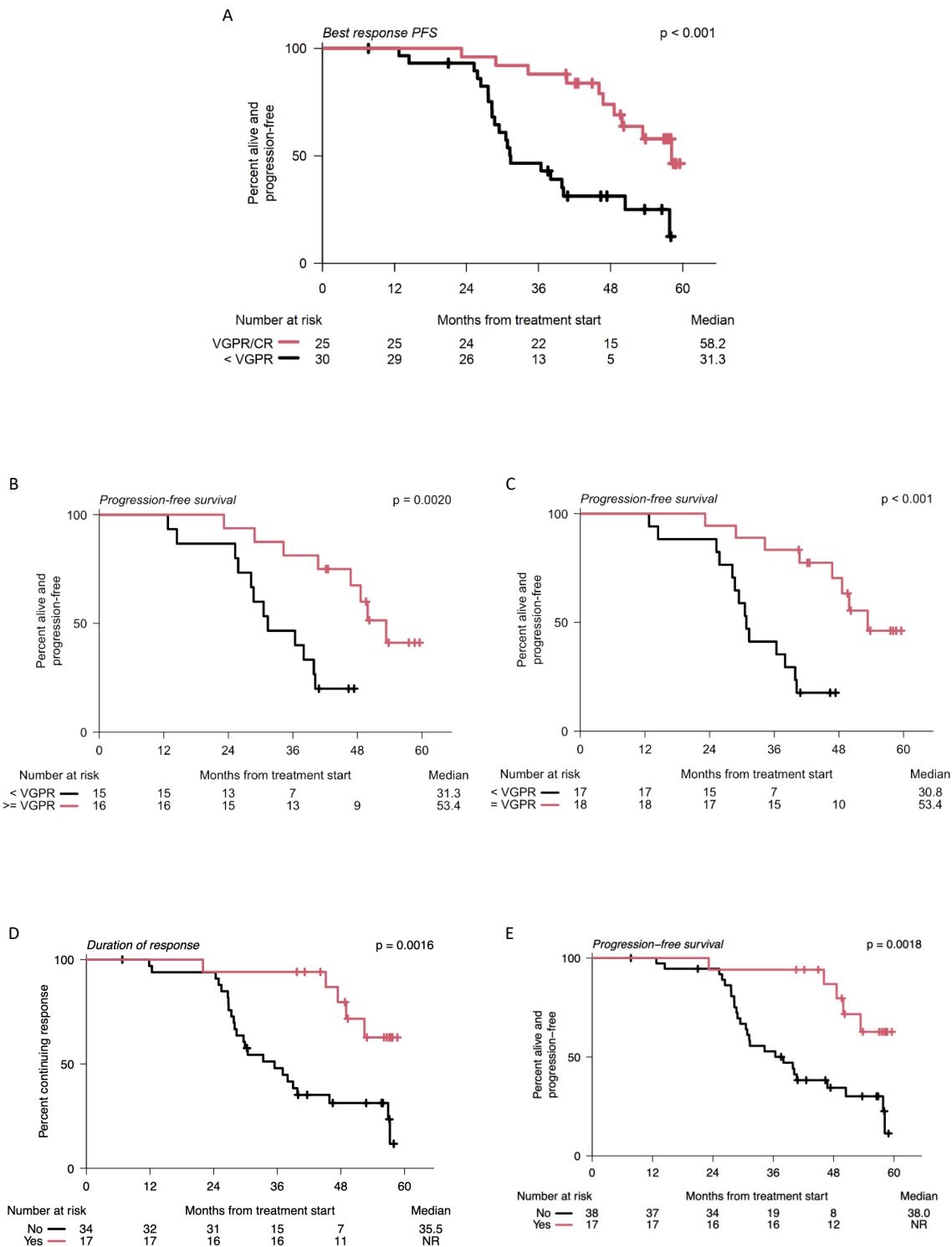


Figure 6

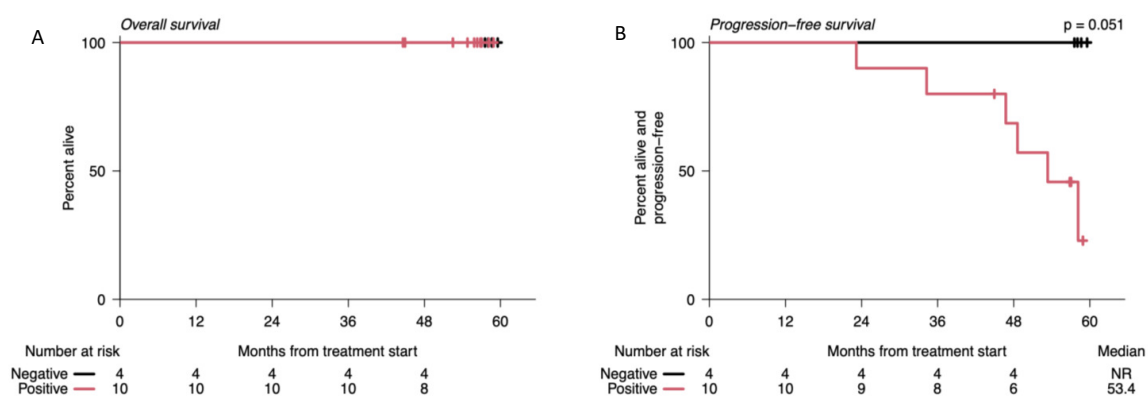


Table 1A. Baseline Characteristics

	(N = 55)
Median age – yr (range)	64 (40-84)
Male sex – no. (%)	30 (55%)
Race – no. / N (%)	
White/Caucasian	53 (96%)
Asian	1 (2%)
Other	1 (2%)
Ethnicity – no. / N (%)	
Hispanic	2 (4%)
Non-Hispanic	53 (96%)
ECOG performance status – no. / N (%)	
0	46 (84%)
1	9 (16%)
Smoldering myeloma disease type – no. / N%	
IgG	37 (67%)
IgA	16 (29%)
Light chain only	2 (4%)
Evolving Disease– no. / N (%)	
Yes	29 (53%)
No	26 (47%)
Cytogenetic risk category – no. / N (%)	
High-risk [t(4;14), t(14;16), del(17p), 1q gain, del1p, del13q]	35 (64%)
Standard-risk	14 (25%)
Not determined	6 (11%)
†Cytogenetic abnormalities - no. / N (%)	
t(4;14)	6 (11%)
t(14;16)	6 (11%)
del(17p)	3 (5%)
1q gain/amp	18 (33%)
t(11;14)	8 (15%)
Monosomy 13	26 (47%)
20/20 Risk	
High	25 (45%)
Intermediate	21 (38%)
Low	9 (16%)
Mayo 2008	
1 risk factor	13 (24%)
2 risk factors	40 (72%)
3 risk factors	2 (4%)

† Cytogenetic abnormalities are compiled from FISH, scRNA-seq and WGS at screening or pre-screening timepoint. For one patient, a primary event translocation was taken from a post-screening timepoint. Cytogenetic data was unknown for 6 patients.

Table 1B. Baseline Risk Stratification

Patient ID	IgA Isotype ^a	M-spike $\geq 3.0^b$	Immuno paresis ^c	FLC Ratio $\geq 8^d$	Evolving Disease ^e	BMPC 50-60% ^f	t(4;14)-17p+1q ^g	High-Risk cytogenetics FISH ^h	High-Risk cytogenetics FISH+Seq ⁱ	Mayo 2008	IMWG 20/2/20	IMWG High Precision	Number of High-Risk Criteria †	Total number of eligibility criteria met (+BMPC $\geq 10\%$) ††
P1	1	0	0	1	1	0	0	0	0	Int	Int	Low-Int	1	3
P2	0	1	1	1	1	1	1	1	1	High	High	High	5	6
P3	1	0	1	0	0	0	0	0	0	Low	Int	Low	0	2
P4	0	0	1	1	1	0	N/A	N/A	0	Int	Low	Low	1	3
P5	0	0	0	1	1	0	0	1	1	Int	High	High	4	2
P6	1	0	0	0	0	0	1	1	1	Low	Low	Low	1	2
P7	1	0	1	0	0	0	0	1	1	Low	Int	Low-Int	1	2
P8	1	0	1	0	0	0	0	0	0	Low	Low	Low	0	2
P9	0	0	1	1	0	0	0	0	1	Int	High	Low-Int	2	2
P10	0	0	1	1	0	1	1	1	1	Int	Int	High	2	4
P11	0	0	1	1	1	0	1	1	1	Int	Int	Int	2	4
P12	1	0	0	0	1	0	1	1	1	Low	Low	Low	2	3
P13	0	0	1	1	0	0	1	1	1	Int	Low	Int	1	3
P14	0	0	1	0	0	0	N/A	N/A	N/A	Low	High	Low-Int	1	1
P15	0	1	0	0	1	1	0	0	0	Int	High	Int	2	3
P16	0	0	0	1	1	0	0	1	1	Int	High	Int	3	2
P17	0	1	0	1	0	1	1	1	1	High	High	High	4	4
P18	0	0	1	1	0	0	0	0	0	Int	High	High	2	2
P19	1	0	1	1	0	0	0	0	0	Int	Int	Int	0	3
P20	0	0	0	1	0	0	N/A	N/A	1	Int	Int	Low-Int	1	1
P21	1	0	0	0	1	0	N/A	N/A	N/A	Low	Low	Low	1	2
P22	0	0	0	1	0	0	1	1	1	Int	High	High	3	2
P23	0	0	0	1	1	0	N/A	N/A	N/A	Int	Low	Low	1	2
P24	0	0	1	1	1	1	1	1	1	Int	High	High	4	5
P25	1	0	1	1	0	1	1	1	1	Int	High	Int	2	5
P26	0	0	0	0	0	0	1	1	1	Low	Low	Low-Int	1	1
P27	0	0	0	1	0	0	0	1	1	Int	Int	Low-Int	1	1
P28	0	0	1	0	1	0	1	1	1	Low	High	Int	3	3
P29	0	0	0	1	1	0	0	0	0	Int	Int	Low-Int	1	2
P30	1	0	1	1	1	1	0	1	1	Int	High	Int	3	5
P31	0	0	1	1	1	0	0	0	0	Int	High	Low-Int	2	3
P32	0	0	1	1	1	1	0	0	1	Int	High	High	4	4
P33	0	0	1	1	1	1	1	1	1	Int	Int	Low-Int	2	5
P34	0	0	0	1	0	0	1	1	1	Int	High	Int	2	2
P35	0	0	0	1	1	0	N/A	N/A	N/A	Int	Int	Low-Int	1	2
P36	0	0	1	1	0	0	1	1	1	Int	Int	Int	1	3
P37	1	0	1	1	1	0	0	0	0	Int	Int	Int	1	4
P38	0	0	1	1	1	0	1	1	1	Int	High	High	4	4
P39	0	0	1	0	0	0	0	0	0	Low	High	Low-Int	1	1
P40	0	0	1	1	1	0	0	1	1	Int	Low	Low-Int	2	3
P41	0	0	0	1	0	0	N/A	N/A	0	Int	Int	Low-Int	0	1
P42	1	0	1	1	1	0	0	1	1	Int	Int	Low-Int	2	4
P43	0	0	0	1	1	0	N/A	N/A	N/A	Int	Int	Low-Int	1	2
P44	0	0	1	1	1	0	0	1	1	Int	Int	Int	2	3
P45	1	0	1	1	1	0	1	1	1	Int	Int	Low-Int	2	5
P46	1	0	1	1	1	0	1	1	1	Int	High	Int	3	5
P47	1	0	0	0	0	0	1	1	1	Low	Int	Low	1	2
P48	0	0	1	0	0	0	0	1	1	Low	Int	Low-Int	1	1
P49	0	0	1	1	1	0	N/A	N/A	N/A	Int	High	Low-Int	2	3
P50	0	0	0	1	1	0	0	1	1	Int	High	Int	3	2
P51	0	0	1	0	0	0	0	0	0	Low	High	Low-Int	1	1
P52	1	0	1	1	0	0	N/A	N/A	N/A	Int	High	Int	1	3
P53	1	0	0	1	0	0	1	1	1	Int	Int	Low-Int	1	3
P54	1	0	0	1	0	0	0	1	1	Int	High	Low-Int	2	2
P55	0	0	0	1	1	0	N/A	N/A	1	Int	High	High	4	2

Abbreviations: FLC, Free Light Chain; BMPC, Bone Marrow Plasma Cells; FISH, Fluorescent In-Situ Hybridization; Seq, Sequencing; Int, Intermediate. Columns ^{a-g} contain high-risk criteria as defined by Rajkumar et al⁴. High-Risk cytogenetics in columns ^{h,i} defined as t(4;14), t(14;16), 1q gain/amp, 13q deletion/monosomy 13, dedeletion 1p, and 17p deletion.

† Total Number of High-Risk Criteria by Mayo 2008, IMWG 20/2/20, IMWG High Precision, Evolving Disease, and High-Risk Cytogenetics by FISH+Seq

†† Total Eligibility criteria met for enrollment as described in Methods section.

Table 2. Summary of Adverse Reactions Reported During Treatment

Event – no. (%)	(N = 55)			
	All grades	Grade 2*	Grade 3*	Grade 4*
Any event	55 (100)	20 (36)	34 (62)	5 (9)
Blood and lymphatic system disorders				
Neutropenia	43 (78)	18 (33)	14 (25)	2 (4)
Thrombocytopenia	33 (60)	4 (7)	4 (7)	1 (2)
Leukopenia	44 (80)	21 (38)	10 (18)	
Anemia	33 (60)	6 (11)	1 (2)	
Lymphopenia	15 (27)	4 (7)	6 (11)	2 (4)
Gastrointestinal disorders				
Diarrhea	27 (67)	5 (9)		
Constipation	26 (47)	1 (2)		
Nausea	33 (60)	3 (5)		
General disorders and administration site conditions				
Fatigue	42 (76)	11 (20)	1 (2)	
Insomnia	31 (56)	3 (5)		
Infections and infestations				
Upper Respiratory Infection	18 (33)	15 (27)	2 (4)	
Investigations				
Alanine aminotransferase increased	14 (25)			
Metabolism and nutrition disorders				
Hypophosphatemia	16 (29)	8 (15)	7 (13)	
Hypomagnesemia	13 (24)			
Hyperglycemia				1 (2)
Hypokalemia	10 (18)		3 (5)	1 (2)
Nervous system disorders	32 (9.0)			
Sensory peripheral neuropathy	31 (56)	7 (13)		
Skin and subcutaneous tissue disorders				
Maculo-papular rash	38 (69)	11 (20)	5 (9)	
Vascular disorders				
Peripheral edema	31 (56)	5 (9)		

* If applicable

Table 3. Summary of Responses to Treatment

	(N = 55)
Best response (IMWG) – no. (%)	
PR or better [95% CI]	51 (93) [84–97]
VGPR or better [95% CI]	25 (45) [32- 56]
CR*	17 (31)
VGPR	8 (15)
PR	26 (47)

*All patients with CR achieved stringent CR